Appendix A.47:

Hurst Pl – CPT 25981

Table 1: Site Description for Hurst Pl (CPT 25981).

Attribute	Yes/No			Description/Date	Symbol in Figure 1
	10-m Buffer	20-m Buffer	50-m Buffer		
Near a body of surface water or other free face features?	No	No	No	The center of the site is ~1000 m to the W from the Pegasus Bay.	NA
Lateral spreading observed during the CES?	No	No	No	Lateral spreading was not observed by the mapping team.[1]	NA
Nearby buildings or structures?	Yes	Yes	Yes	Building coverage of the 10-, 20-, and 50-m buffers is 18, 22, and 28%, respectively. The buildings are in all quadrants of the buffers.	White Fill + Brown Outline
Sloping land?	No	No	No	Flat land, residential area	NA
Step changes in the ground surface?	No	No	No	NA	NA
Retaining walls?	No	No	No	NA	NA
Vegetation?	Yes	Yes	Yes	Trees and bushes cover 29, 47, and 27% of the 10-, 20-, and 50-m buffers, respectively. They are in all quadrants of the buffers.	White Fill + Green Outline
Anthropogenic changes to the site between the LiDAR surveys?	Yes	Yes	Yes	New parking lot pavement between Apr 2005 and Feb 2006 in the N portion of the 50-m buffer). Minor vegetation removal in the SW quadrant of all buffers between Mar 2009 and 3 Sep 2010. Road (Hurst Pl) re-construction between Dec 2011 and Apr 2012 in the SE q. of the 50-m buffer. Land releveling in all quadrants of all buffers was conducted between Apr 2012 and Jan 2013. Building replacement between Jan 2015 and Jun 2015 in the SW q. of the 50-m buffer. Between Sep 2015 and Nov 2015, building removal in the SE q. of the 50-m buffer and road re-construction in the SE q. of the 50-m buffer.	Vegetation Removal: Green Crossline; Building Addition/ Removal: Orange Crossline
Other important factors?	No	No	Yes	Low-motor-vehicle-volume road (Hurst Pl) occupies 5% of the 50-m buffer in its SE quadrant.	Road: Gray Fill + Red Outline

Note: Buffer is the area within a circle of a specified radius with CPT investigations done at its center (172.709763°, -43.481524°).

[1] Canterbury Geotechnical Database. (2012). "Observed Ground Crack Locations", Map Layer CGD0400 - 23 July 2012, retrieved July 09, 2018 from https://canterburygeotechnicaldatabase.projectorbit.com/

Figure 1: Site plan with areas where ejecta-induced settlement is considered.

Note 1: Patch A in the free field was selected for settlement assessment as an area free of vegetation and structures. Other important factors considered in the patch selection process were its proximity to a CPT, a property subjected to addition and/or demolition of a structure, front yard/backyard alterations (e.g., ploughing, rubble, scrap), aerial distribution of sediment ejecta, and the availability of LDAT property inspection notes. In addition, the entire portion of the road within the 50-m buffer was considered for the settlement assessment. The LiDAR-based settlement analyses were not conducted for this site due to the unavailability of the Sep-10 LiDAR survey used to compute the ground surface subsidence for the Sep-10 and Feb-11 EQs and the uncertainties associated with LiDAR measurements for the Jun-11 and Dec-11 EQs (Table 2).

Table 2: LiDAR flight error adjustments, global adjustments for the difference between average LiDAR point elevations and benchmark survey elevations, and vertical tectonic movement adjustments.

	Adjustments (mm)		
Earthquake Event(s)	LiDAR Flight Error	Global Offset[2]	Tectonic Vertical Movement
Sep-10	NA	-3	0
Feb-11	NA	16	-30
Jun-11	-100	38	-40
Dec-11	+100	-65	-10
CES	-50	-14	-80
Any LiDAR survey affected by ejecta?			No

Note: The negative sign indicates the subtraction from the ground surface subsidence, while the positive sign indicates the addition to the ground surface subsidence.

Table 3a: LiDAR Measurement Error for Patch A.

Surveys	Buffer	Area Averaged Difference Indicating Repeat Measurement Error (mm)	$\sigma^*_{\text{individual LiDAR points}}$ (mm)	%Reduction in σ due to Area Averaging of LiDAR Points
Post Feb 2011: Mar 2011 and May 2011	10-m	ND	59	[ND,ND]
	20-m	ND		
	50-m	ND		
Post Dec 2011: Feb 2012 and Oct 2015	10-m	ND	70	[ND,ND]
	20-m	ND		
	50-m	ND		

*Standard deviation; ND = Not determined.

[2] Russell, J., & van Ballegooy, S. (2015). *Canterbury Earthquake Sequence: Increased liquefaction vulnerability assessment methodology*. New Zealand: Tonkin & Taylor Ltd.

Table 3b: LiDAR Measurement Error for Road.

Surveys	Buffer	Area Averaged Difference Indicating Repeat Measurement Error (mm)	$\sigma^*_{\text{individual LiDAR points}}$ (mm)	%Reduction in σ due to Area Averaging of LiDAR Points
Post Feb 2011: Mar 2011 and May 2011	10-m	NA	59	[ND,ND]
	20-m	NA		
	50-m	ND		
Post Dec 2011: Feb 2012 and Oct 2015	10-m	NA	70	[ND,ND]
	20-m	NA		
	50-m	ND		

*Standard deviation; ND = Not determined.

Table 4a: Ground surface subsidence adjustments due to LiDAR measurement error for Patch A.

Earthquake Event(s)	$\sigma_{\text{pre-EQ LiDAR survey}}$ (mm)	$\sigma_{\text{post-EQ LiDAR survey}}$ (mm)	σ_{total} (mm)	Area Average Adjusted σ (mm) **
Sep-10	158	56	134	ND
Feb-11	56	59	59	ND
Jun-11	59	61	62	ND
Dec-11	61	70	87	ND
CES	158	70	124	ND

**Based on the highest %Reduction in Table 3a.

Table 4b: Ground surface subsidence adjustments due to LiDAR measurement error for Road.

Earthquake Event(s)	$\sigma_{\text{pre-EQ LiDAR survey}}$ (mm)	$\sigma_{\text{post-EQ LiDAR survey}}$ (mm)	σ_{total} (mm)	Area Average Adjusted σ (mm) **
Sep-10	158	56	134	ND
Feb-11	56	59	59	ND
Jun-11	59	61	62	ND
Dec-11	61	70	87	ND
CES	158	70	124	ND

**Based on the highest %Reduction in Table 3d.

Table 5a: Raw liquefaction-related ground surface subsidence using original LiDAR points for Patch A.

	Average Ground Surface Subsidence (mm)		
Earthquake Event(s)	10-m Buffer	20-m Buffer	50-m Buffer
Sep-10	NA	NA	NA
Feb-11	NA	NA	NA
Jun-11	ND	ND	ND
Dec-11	ND	ND	ND
CES	ND	ND	ND

NA = Not available; ND = Not determined.

Table 5b: Raw liquefaction-related ground surface subsidence using original LiDAR points for Road.

	Average Ground Surface Subsidence (mm)		
Earthquake Event(s)	10-m Buffer	20-m Buffer	50-m Buffer
Sep-10	NA	NA	NA
Feb-11	NA	NA	NA
Jun-11	ND	ND	ND
Dec-11	ND	ND	ND
CES	ND	ND	ND

NA = Not available; ND = Not determined.

Table 6a: Corrected liquefaction-related ground surface subsidence using original LiDAR points for Patch A with the calculated adjustments in Table 2.

	Average Calculated Ground Surface Subsidence (mm)		
Earthquake Event(s)	10-m Buffer	20-m Buffer	50-m Buffer
Sep-10	NA	NA	NA
Feb-11	NA	NA	NA
Jun-11	ND	ND	ND
Dec-11	ND	ND	ND
CES	ND	ND	ND

Notes: Plus/minus values are same as those in Table 4a, but rounded to the nearest 25 mm; Positive overall values indicate ground surface subsidence, while negative overall values indicate ground surface uplift; NA = Not available; ND = Not determined.

Table 6b: Corrected liquefaction-related ground surface subsidence using original LiDAR points for Road with the calculated adjustments in Table 2.

	Average Calculated Ground Surface Subsidence (mm)		
Earthquake Event(s)	10-m Buffer	20-m Buffer	50-m Buffer
Sep-10	NA	NA	NA
Feb-11	NA	NA	NA
Jun-11	ND	ND	ND
Dec-11	ND	ND	ND
CES	ND	ND	ND

Notes: Plus/minus values are same as those in Table 4c, but rounded to the nearest 25 mm; Positive overall values indicate ground surface subsidence, while negative overall values indicate ground surface uplift; NA = Not available; ND = Not determined.

Table 7a: Corrected liquefaction-related ground surface subsidence for Patch A using LiDAR DEMs.

	Estimated Ground Surface Subsidence (mm)								
	10-m Buffer			20-m Buffer			50-m Buffer		
Earthquake Event(s)	16^{th} %ile	50^{th} %ile	84^{th} %ile	16^{th} %ile	50^{th} %ile	84^{th} %ile	16^{th} %ile	50^{th} %ile	84^{th} %ile
Sep-10	NA	NA	NA	NA	NA	NA	NA	NA	NA
Feb-11	NA	NA	NA	NA	NA	NA	NA	NA	NA
Jun-11	<50	<50	50	<50	<50	50	<50	<50	50
Dec-11	100	100	150	100	100	150	100	100	150
CES	200	300	350	200	300	350	200	300	350

Note: These percentiles are not the exact statistical measures; they indicate the spatial variability of ground surface subsidence.

Table 7b: Corrected liquefaction-related ground surface subsidence for Road using LiDAR DEMs.

	Estimated Ground Surface Subsidence (mm)								
	10-m Buffer			20-m Buffer			50-m Buffer		
Earthquake Event(s)	16^{th} %ile	50^{th} %ile	84^{th} %ile	16^{th} %ile	50^{th} %ile	84^{th} %ile	16^{th} %ile	50^{th} %ile	84^{th} %ile
Sep-10	NA	NA	NA	NA	NA	NA	NA	NA	NA
Feb-11	NA	NA	NA	NA	NA	NA	NA	NA	NA
Jun-11	NA	NA	NA	NA	NA	NA	<50	50	50
Dec-11	NA	NA	NA	NA	NA	NA	100	100	150
CES	NA	NA	NA	NA	NA	NA	150	200	250

Note: These percentiles are not the exact statistical measures; they indicate the spatial variability of ground surface subsidence.

Table 8a: Ejecta-Induced settlement for the top 20 m of the soil profile for Patch A for the 50th %ile PGA, P_L=50%, and C_{FC}=0.13 using BI-2014, ZRB-2002, and I_C cutoff of 2.6.

Earthquake Event(s)	M_W	PGA (g)	Depth to Groundwater (m)	S_T (mm)	S_{V1D} (mm)	$S_{E,L}$ (mm)
Sep-10	7.1	0.18	1.5	NA	32±20	NA
Feb-11	6.2	0.40	1.5	NA	92±50	NA
Jun-11	6.2	0.20	1.5	ND	38±25	ND
Dec-11	6.1	0.35	1.5	ND	83±50	ND

Notes: S_T = Total settlement (Table 6); S_{V1D} = Average vertical settlement due to volumetric compression using Boulanger and Idriss (2014) (BI-2014), Zhang et al. (2002) (ZRB-2002) procedures and de Greef and Lengkeek (2018) thin-layer correction; $S_{E,L}$ = Ejecta-induced settlement as the difference between the LiDAR-based S_T and S_{V1D}.

Table 8b: Ejecta-Induced settlement for the top 20 m of the soil profile for Road (50-m buffer) for the 50th %ile PGA, P_L=50%, and C_{FC}=0.13 using BI-2014, ZRB-2002, and I_C cutoff of 2.6.

Earthquake Event(s)	M_W	PGA (g)	Depth to Groundwater (m)	S_T (mm)	S_{V1D} (mm)	$S_{E,L}$ (mm)
Sep-10	7.1	0.18	1.5	NA	8±20	NA
Feb-11	6.2	0.40	1.5	NA	76±50	NA
Jun-11	6.2	0.20	1.5	ND	6±25	ND
Dec-11	6.1	0.35	1.5	ND	56±50	ND

Notes: S_T = Total settlement (Table 6); S_{V1D} = Average vertical settlement due to volumetric compression using Boulanger and Idriss (2014) (BI-2014), Zhang et al. (2002) (ZRB-2002) procedures and de Greef and Lengkeek (2018) thin-layer correction; $S_{E,L}$ = Ejecta-induced settlement as the difference between the LiDAR-based S_T and S_{V1D}.

Note 3: The uncertainty for volumetric settlement was derived based on the sensitivity of volumetric settlement to PGA, C_{FC}, and P_L for each earthquake event for VsVp 57203 *Shirley Intermediate School* and CC LIQ 1 – CPT 5586 – *Vivian St* sites. Taking the 50th percentile as the baseline case, the minimum and maximum values corresponding to the difference between the 25th percentile and the 50th percentile and the 75th percentile and the 50th percentile were determined. The arithmetic mean of the range of the minimum and maximum difference was evaluated for each patch at the two sites. The maximum arithmetic mean for each earthquake event was rounded to the nearest five and used as the uncertainty value. Accordingly, the 1-D volumetric settlement uncertainties of ±20, ±50, ±25, and ±50 mm for the Sep-10, Feb-11, Jun-11, and Dec-11 earthquake events, respectively, were used for all sites in this study.

Table 9a: Coverage area and height of ejecta estimates for Patch A (10-, 20-, and 50-m buffers) using photographs.

EQ Event	$H_{E,thick1}$ (mm)	$A_{E,thick1}$ (m^2)	$H_{E,thick2}$ (mm)	$A_{E,thick2}$ (m^2)	$H_{E,thin1}$ (mm)	$A_{E,thin1}$ (m^2)	$H_{E,thin2}$ (mm)	$A_{E,thin2}$ (m^2)	A_T (m^2)
Sep-10	0	0	0	0	0	0	0	0	125
Feb-11	100-150	33.1	60-100	23.9	40-60	26.2	5-10	32.1	125
Jun-11*	0	0	30-60	64.7	0	0	0	0	108**
Dec-11	120-180	6.0	40-60	13.9	30-50	48.2	5-10	9.8	122**

Notes: $A_{E,thick/thin}$ =Coverage area of thick/thin ejecta layers; $H_{E,thick/thin}$ = Lower-upper estimate of height of thick/thin ejecta layers; A_T= Total assessment area of a buffer being considered; * indicates uncertainty due to the presence of shadows; ** indicates reduction in A_T due to the presence of shadows/objects.

Table 9b: Coverage area and height of ejecta estimates for Road (50-m buffer) using photographs.

EQ Event	$H_{E,cc}$ (mm)	$V_{E,cc}$ (m^3)	$H_{E,prism/pyr}$ (mm)	$V_{E,prism+pyr}$ (m^3)	$H_{E,thick}$ (mm)	$A_{E,thick}$ (m^2)	$H_{E,thin}$ (mm)	$A_{E,thin}$ (m^2)	A_T (m^2)
Sep-10	0	0	0	0	0	0	0	0	357
Feb-11	202-1686	16.0	15-150	1.98-3.75	0	0	3-6	264	357
Jun-11	0	0	0	0	30-60	296	2-4	61.0	357
Dec-11	ND	ND	ND	ND	ND	ND	ND	ND	357

Notes: $H_{E,cc}$ = Lower-upper estimate of height of conically shaped ejecta pile components (based on the repose angle of 30°); $V_{E,cc}$ = Volume of conically shaped ejecta pile components; $H_{E,prism/pyr}$ = Lower-upper estimate of ejecta height near the curb based on 2-4% cross slope of normal crown; $V_{E,prism+pyr}$ = Lower-upper estimate of total volume of prismatic- and pyramidal-shape ejecta; $A_{E,thick/thin}$ =Coverage area of thick/thin ejecta layers; $H_{E,thick/thin}$ = Lower-upper estimate of height of thick/thin ejecta layers; A_T = Total assessment area of a buffer being considered; ND = Not determined due to the uncertainty in the place of origin of the ejecta pile whose volume is ~40 m^3 and many cars covering potential ejecta.

Note 3: The values in Table 9 correspond to the coverage area of ejecta outlined in aerial photographs (Figures 9, 10, and 39-41) and the lower and upper estimates of ejecta height based on geometrical approximations, ground photographs (Figures 43 and 44), and EQC LDAT property inspection reports (e.g., Figure 42). The ejecta-induced settlement using photographs and engineering judgment, $S_{E,P}$, is estimated as

$$S_{E,P} = \frac{\sum_{i=1}^{a} A_{E,thick,i} * H_{E,thick,i} + \sum_{j=1}^{b} A_{E,thin,j} * H_{E,thin,j} + \frac{1}{3}\sum_{k=1}^{c} A_{E,pile,k} * R_{E,pile,k} * tan30°}{A_T} + \frac{\frac{1}{2}\sum_{n=1}^{f} W_{E,prism,n} * H_{E,prism,n} * L_{E,prism,n} + \frac{1}{3}\sum_{p=1}^{g} W_{E,r.pyramid,p} * H_{E,r.pyramid,p} * L_{E,r.pyramid,p}}{A_T} + \frac{\frac{1}{6}\sum_{r=1}^{h} W_{E,t.pyramid,r} * H_{E,t.pyramid,r} * L_{E,t.pyramid,r}}{A_T} = \frac{\sum_{i=1}^{a} V_{E,thick,i} + \sum_{j=1}^{b} V_{E,thin,j} + \sum_{k=1}^{c} V_{E,conical\ component,k}}{A_T} + \frac{\sum_{n=1}^{f} V_{E,prism,n} + \sum_{p=1}^{g} V_{E,r.pyramid,p} + \sum_{r=1}^{h} V_{E,t.pyramid,r}}{A_T}$$

where

- $A_{E,thick,i}$ and $H_{E,thick,i}$ are the area and the height of a thick ejecta layer, respectively;
- $A_{E,thin,j}$ and $H_{E,thin,j}$ are the area and the height of a thin ejecta layer, respectively;
- $A_{E,pile,k}$ and $R_{E,pile,k}$ are the area and the radius of an ejecta pile component, respectively, shaped as a cone with the repose angle of 30°;
- $W_{E,prism,n}$ and $L_{E,prism,n}$ are the width and the length, respectively, of the coverage area of a prismatically shaped ejecta layer, and $H_{E,prism,n}$ is the height of the prism-like ejecta layer;
- $W_{E,r.pyr,p}$ and $L_{E,r.pyr,p}$ are the width and the length, respectively, of the coverage area of an ejecta layer shaped as a pyramid with the rectangular base, and $H_{E,r.pyr,p}$ is the height of the rectangular-base pyramid-like ejecta layer;
- $W_{E,t.pyr,r}$ and $L_{E,t.pyr,r}$ are the width and the length, respectively, of the coverage area of an ejecta layer shaped as a pyramid with the triangular base, and $H_{E,r.pyr,p}$ is the height of the triangular-base pyramid-like ejecta layer;
- A_T is the total assessment area for a buffer being considered (Figure 1).

Table 10: Ejecta-induced settlement estimates for Patch A and Road based on photographs.

Earthquake Event	Patch A (10-, 20-, and 50-m buffers)		Road (50-m buffer)	
	$S_{E,P,lower}$ (mm)	$S_{E,P,upper}$ (mm)	$S_{E,P,lower}$ (mm)	$S_{E,P,upper}$ (mm)
Sep-10	0	0	0	0
Feb-11	48	74	52	60
Jun-11	18*	36*	25	50
Dec-11	23	36	ND	ND

Note: $S_{E,P,lower}$ and $S_{E,P,upper}$ correspond to lower and upper estimates of $S_{E,P}$, respectively; * indicates uncertainty due to the presence of shadows; ND = Not determined due to the uncertainty in the place of origin of the ejecta pile.

Table 11: Best final estimates of ejecta-induced settlement for Patch A and Road.

Earthquake Event	Patch A (10-, 20-, and 50-m buffers)			Road (50-m buffer)		
	$S_{E,L}$ (mm)	$S_{E,P}$ (mm)	$S_{E,final}$ (mm)	$S_{E,L}$ (mm)	$S_{E,P}$ (mm)	$S_{E,final}$ (mm)
Sep-10	NA	0	0	NA	0	0
Feb-11	NA	61±13	60±15	NA	56±4	55±5
Jun-11	ND	27±9	*25±10	ND	38±12	40±10
Dec-11	ND	30±6	30±5	ND	ND	ND

Notes: $S_{E,L}$ = Ejecta-induced settlement based on LiDAR data reported in Table 8; $S_{E,P}$ = Median ejecta-induced settlement for the range of values reported in Table 10; $S_{E,final}$ = Best final estimate of ejecta-induced settlement rounded to the nearest 5 mm; Final plus/minus values are also rounded to the nearest 5 mm; * indicates uncertainty due to the presence of shadows; NA = Not available; ND = Not determined.

Note 4:

- Patch A and Road: $S_{E,final}$ is based solely on $S_{E,P}$ for all earthquake events (please see Note 1 and Table 2 for the explanation).
- The LDAT inspection report and ground photographs from July 2011 are available for the property with Patch A. The ejecta height was not recorded because nearly all ejecta were removed from the property at the time of the inspection (July 2011). The ejecta height at another property within the 50-m buffer was measured as 300 mm. There are no ground photographs of ejecta on the road.
- The Hurst Pl site is in the zone of slight LPI overprediction of liquefaction severity for the Sep-10 EQ and accurate LPI prediction of liquefaction severity for the Feb-11 EQ (Maurer et al. 2014[3]).

Summary 1:

- **The best estimate of the ejecta-induced free-field ground settlement at the Hurst Pl site for the SEP 2010, FEB 2011, JUN 2011, and DEC 2011 earthquake is 0 mm, 60±15 mm, 25±10 mm, and 30±5 mm, respectively.**
- **The best estimate of the ejecta-induced free-field ground settlement of the road at the Hurst Pl site for the SEP 2010, FEB 2011, and JUN 2011earthquake is 0 mm, 55±5 mm, and 40±10 mm, respectively. The ejecta-induced settlement for the DEC 2011 EQ could not be estimated with confidence.**

[3] Maurer, B. W., Green, R. A., Cubrinovski, M., & Bradley, B. A. (2014). Evaluation of the Liquefaction Potential Index for Assessing Liquefaction Hazard in Christchurch, New Zealand. *Journal of Geotechnical and Geoenvironmental Engineering*, 140(7), 04014032-1-11. doi:10.1061/(asce)gt.1943-5606.0001117

Figure 2: Location of the site.

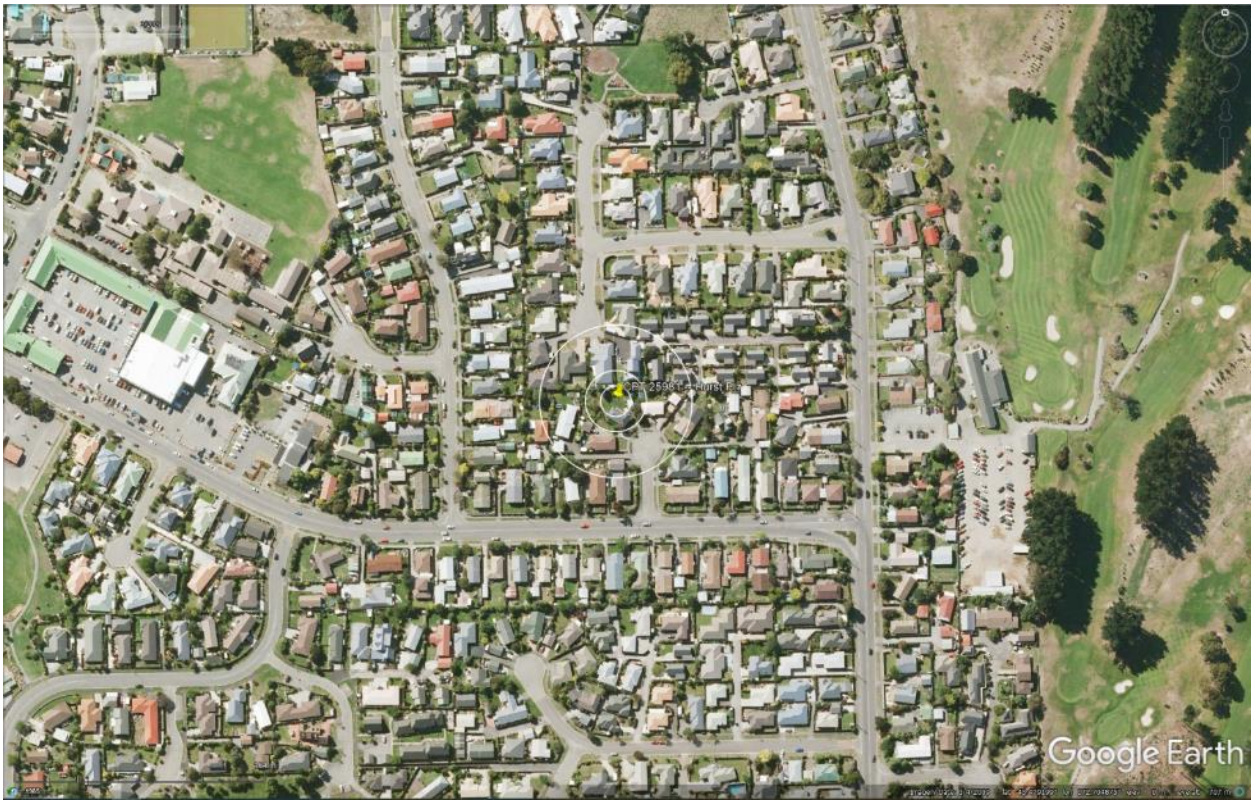

Figure 3: Position of the site relative to nearby buildings, vegetation, and free-face features.

Figure 4: Street view of the flat land.

Figure 5: Satellite image of the site taken in Dec 2004.

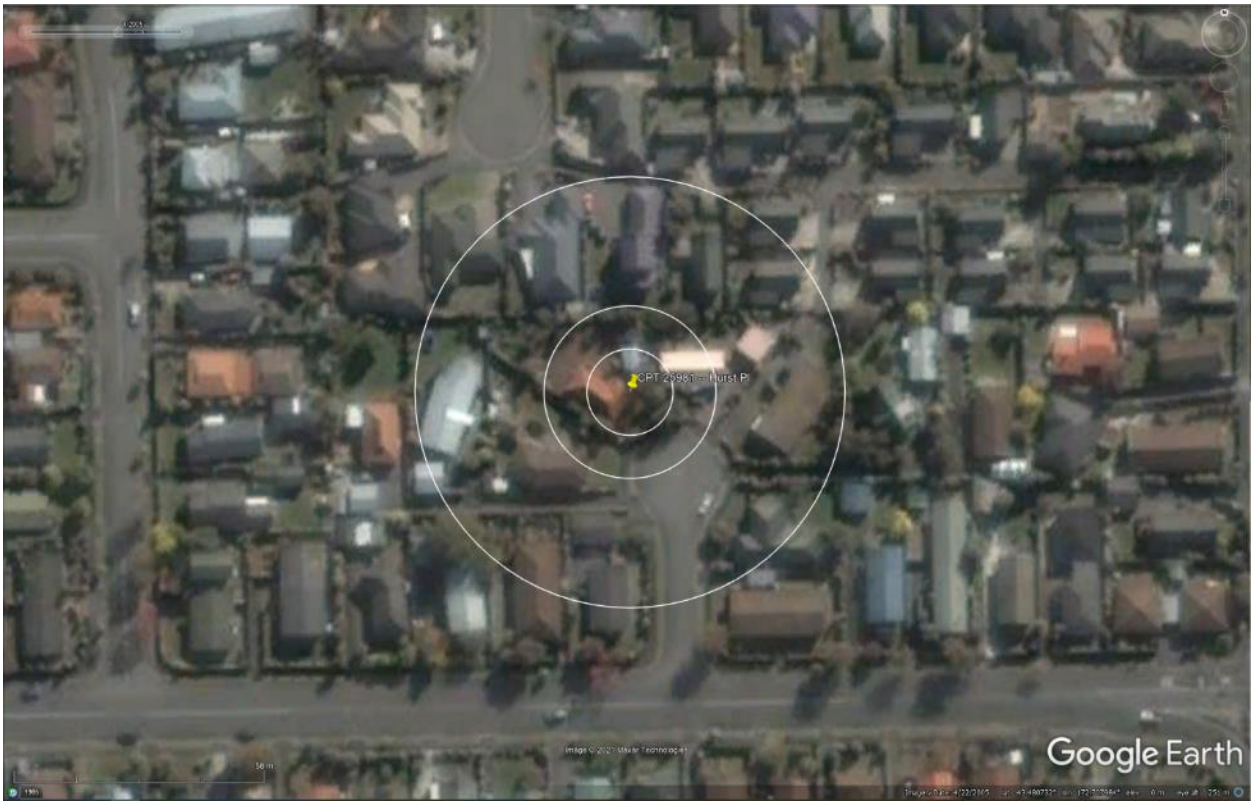

Figure 6: Satellite image of the site taken in Apr 2005.

Figure 7: Satellite image of the site taken in Feb 2006.

Figure 8: Satellite image of the site taken in Mar 2009.

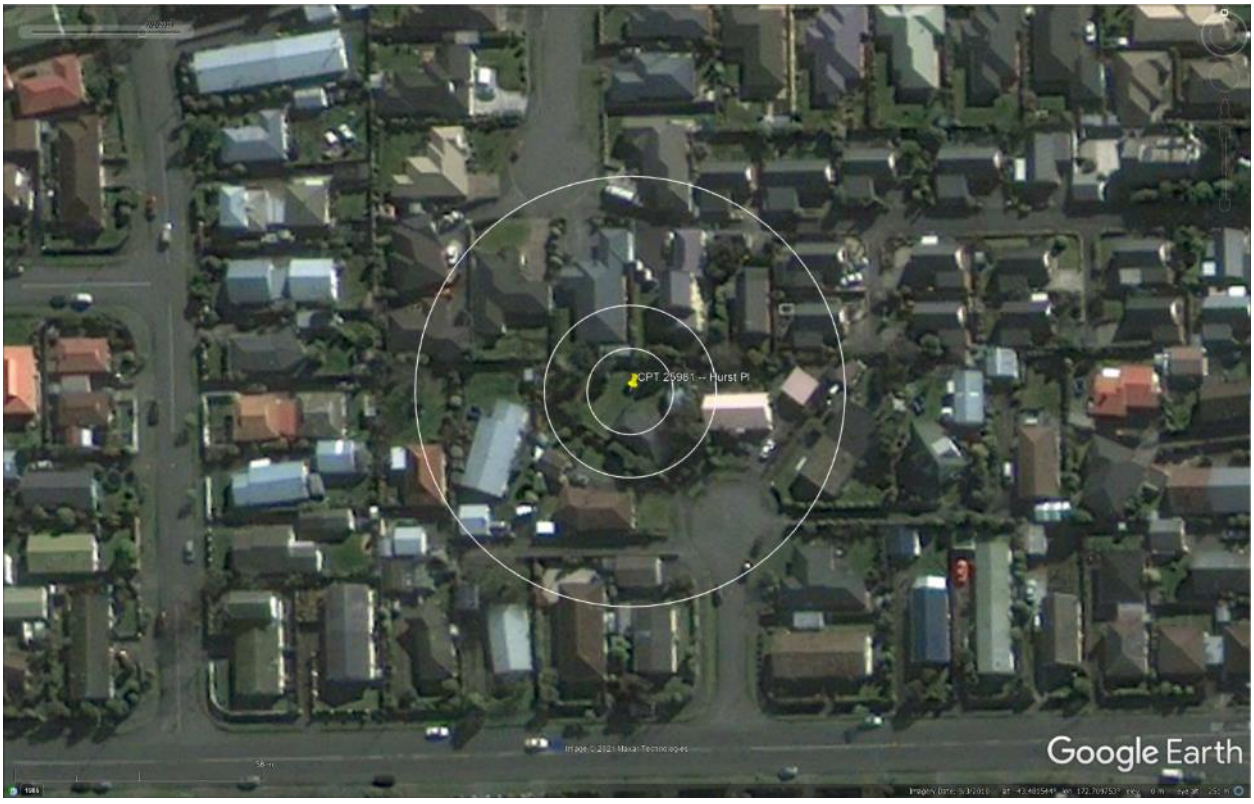

Figure 9: Satellite image of the site taken on Sep 3, 2010.

Figure 10: Satellite image of the site taken on Sep 5, 2010.

Figure 11: Satellite image of the site taken on Feb 7, 2011.

Figure 12: Satellite image of the site taken on Feb 23, 2011.

Figure 13: Satellite image of the site taken on Feb 26, 2011.

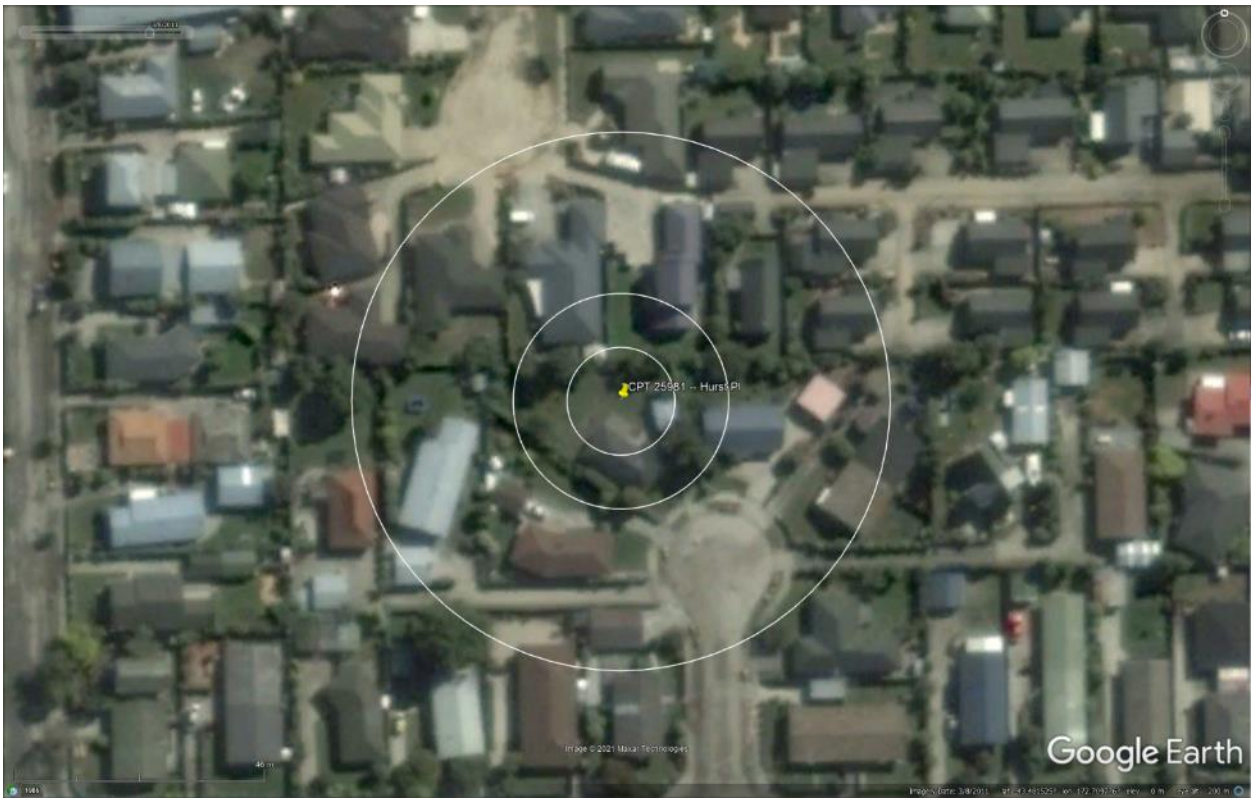

Figure 14: Satellite image of the site taken on Mar 8, 2011.

Figure 15: Satellite image of the site taken in Apr 2012.

Figure 16: Satellite image of the site taken in Jan 2013.

Figure 17: Satellite image of the site taken in Jan 2015.

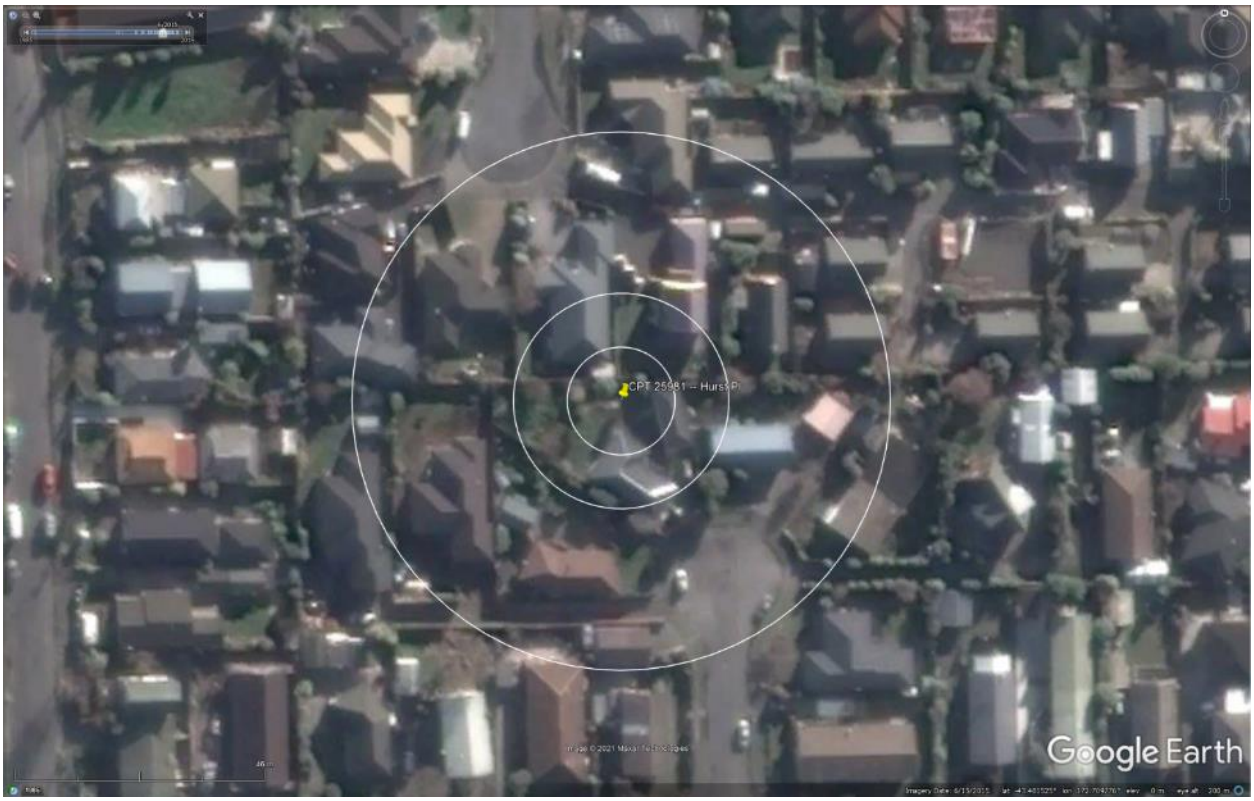

Figure 18: Satellite image of the site taken in Jun 2015.

Figure 19: Satellite image of the site taken in Sep 2015.

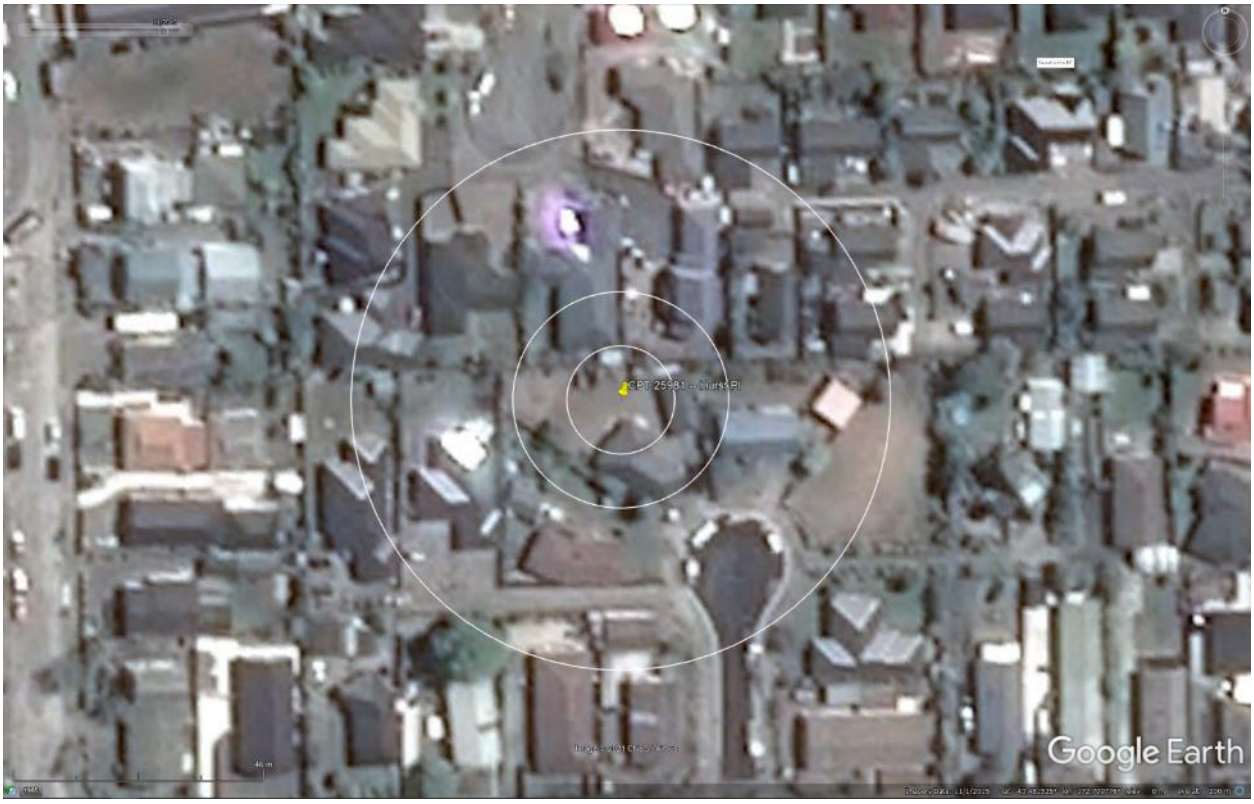

Figure 20: Satellite image of the site taken in Nov 2015.

Figure 21: Aerial photograph of the site taken on Sep 4, 2010.

Figure 22: Aerial photograph of the site taken on Feb 24, 2011.

Figure 23: Aerial photograph of the site taken on June 14-15, 2011.

Figure 24: Aerial photograph of the site taken on June 16, 2011.

Figure 25: Aerial photograph of the site taken on Dec 24, 2011.

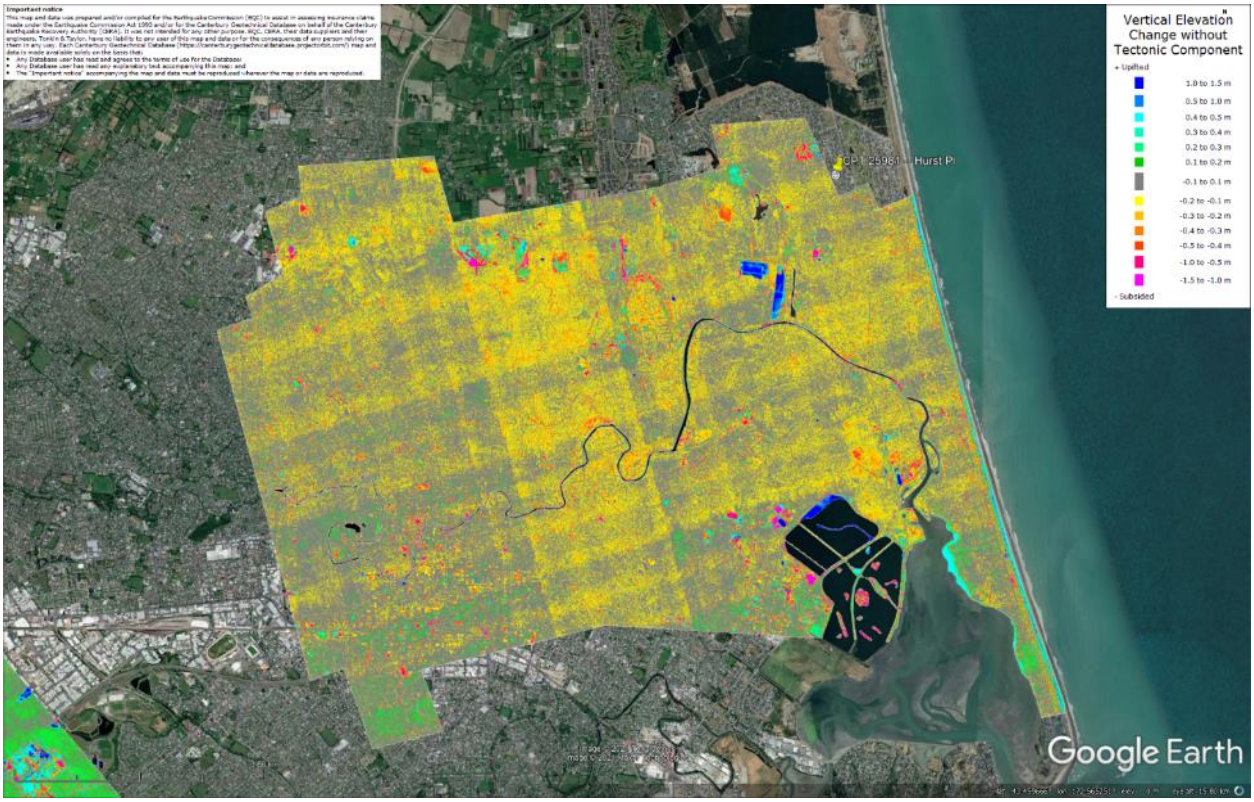

Figure 26: Vertical Ground Movements (Surface – Tectonic) for Sep 2010 Earthquake are not available for the site. It is, however, evident that the site is in the apparent zone of overestimated ground surface subsidence (i.e., July 2003 LiDAR flight band error).

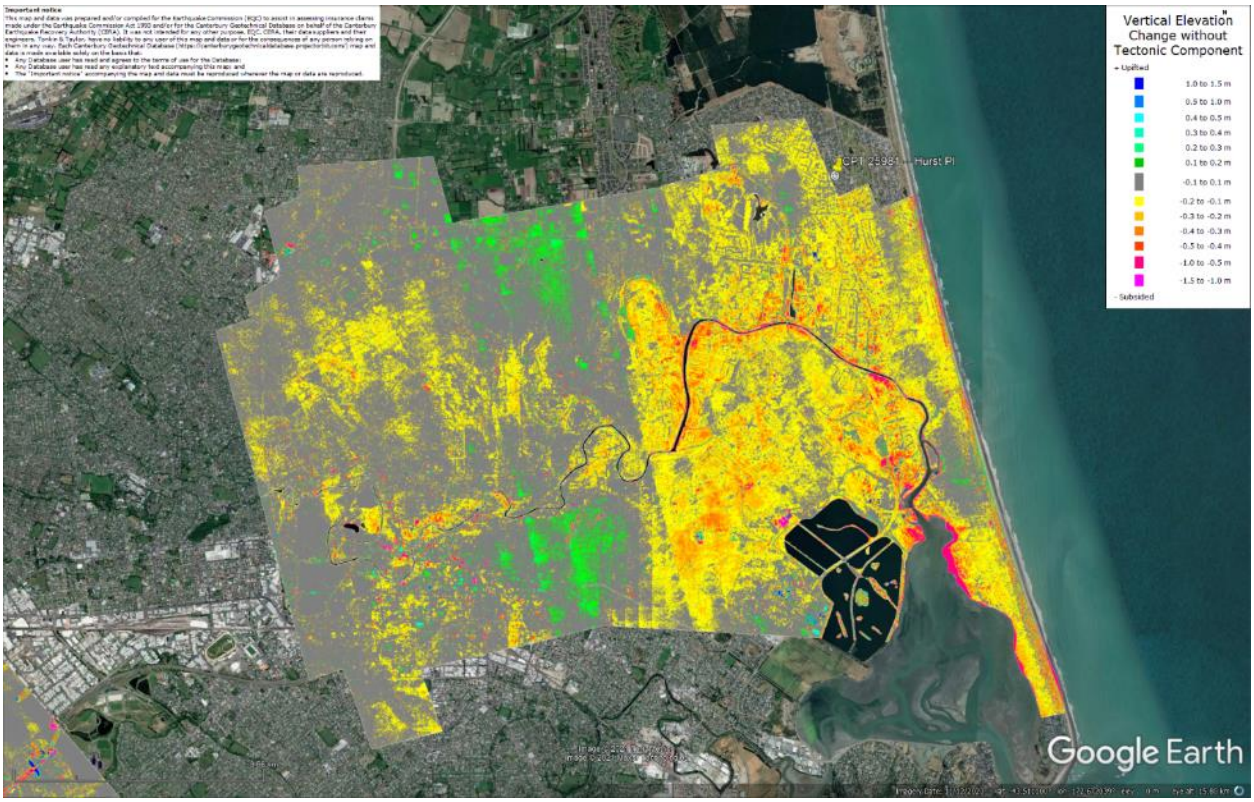

Figure 27: Vertical Ground Movements (Surface – Tectonic) for Feb 2011 Earthquake are not available for the site.

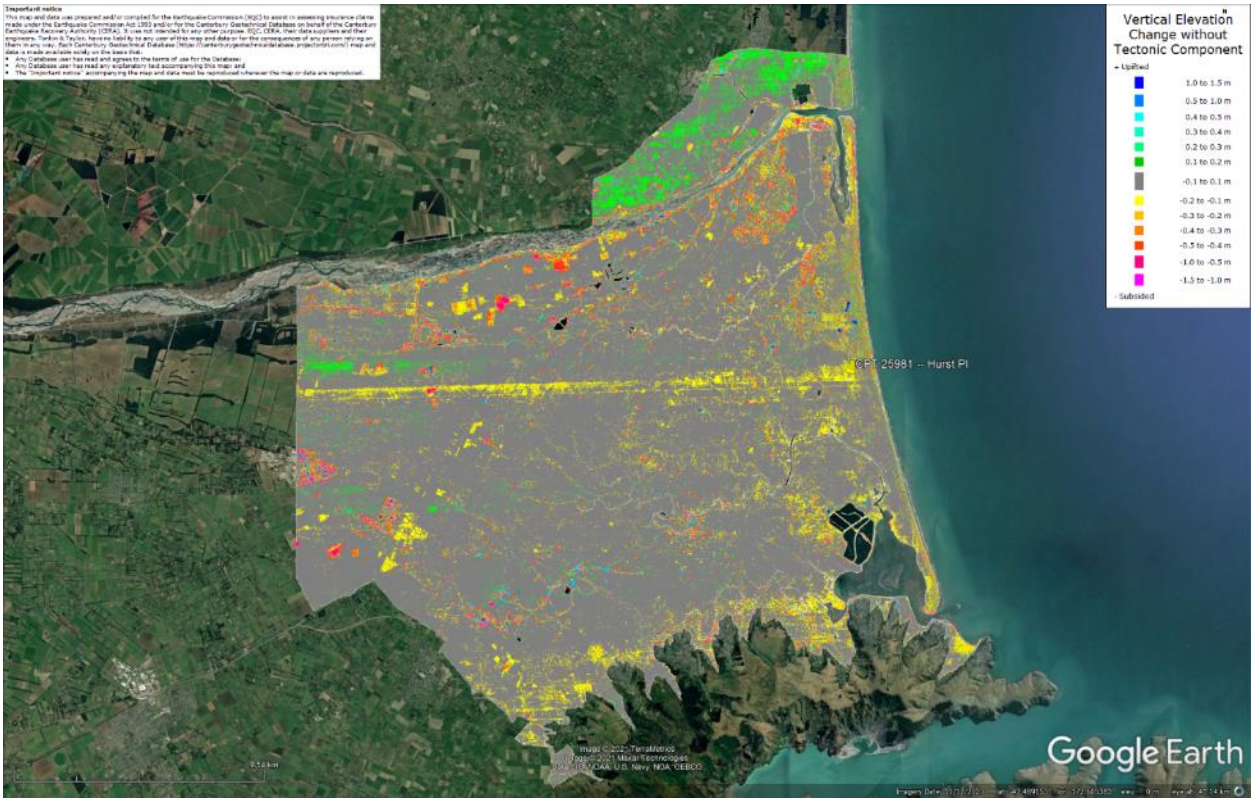

Figure 28: Vertical Ground Movements (Surface – Tectonic) for June 2011 Earthquake – the site is in the apparent zone of overestimated ground surface subsidence (i.e., Sep 2011 LiDAR flight band error).

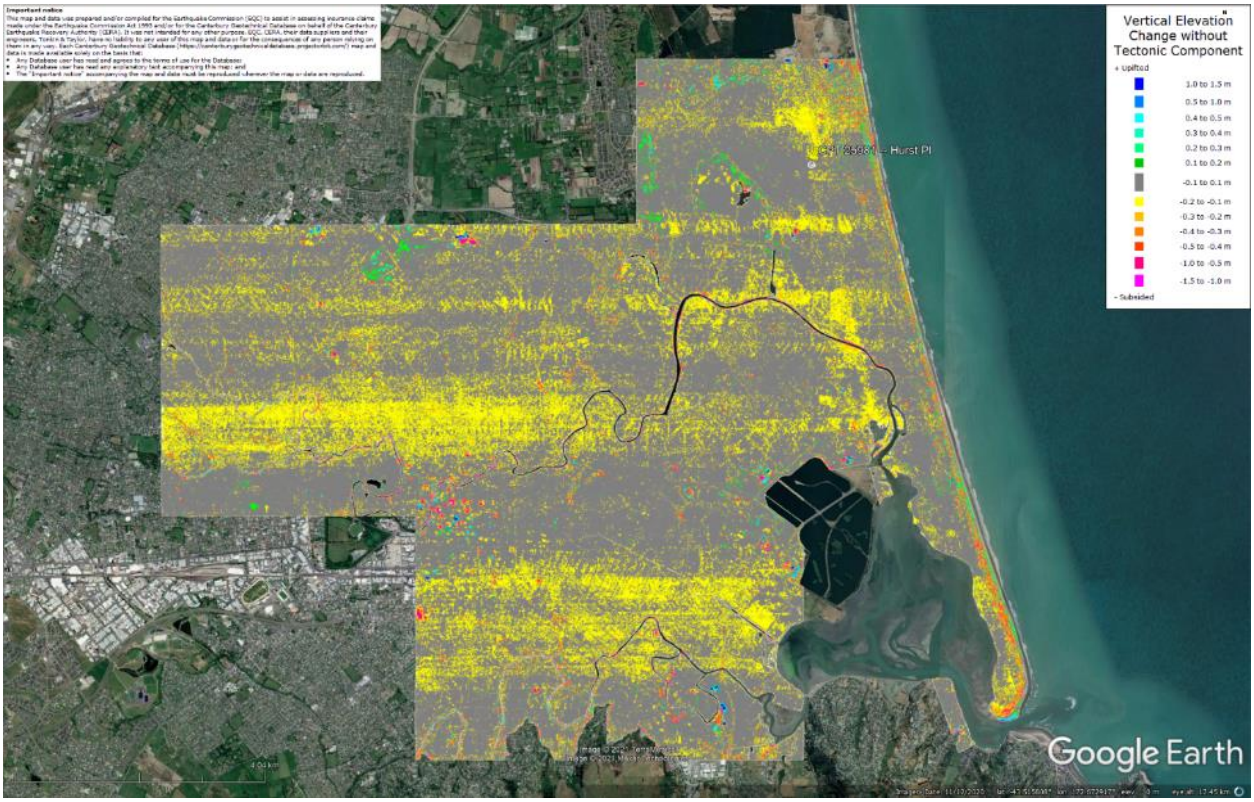

Figure 29: Vertical Ground Movements (Surface – Tectonic) for Dec 2011 Earthquake – the site is in the apparent zone of underestimated ground surface subsidence (i.e., Sep 2011 LiDAR flight band error).

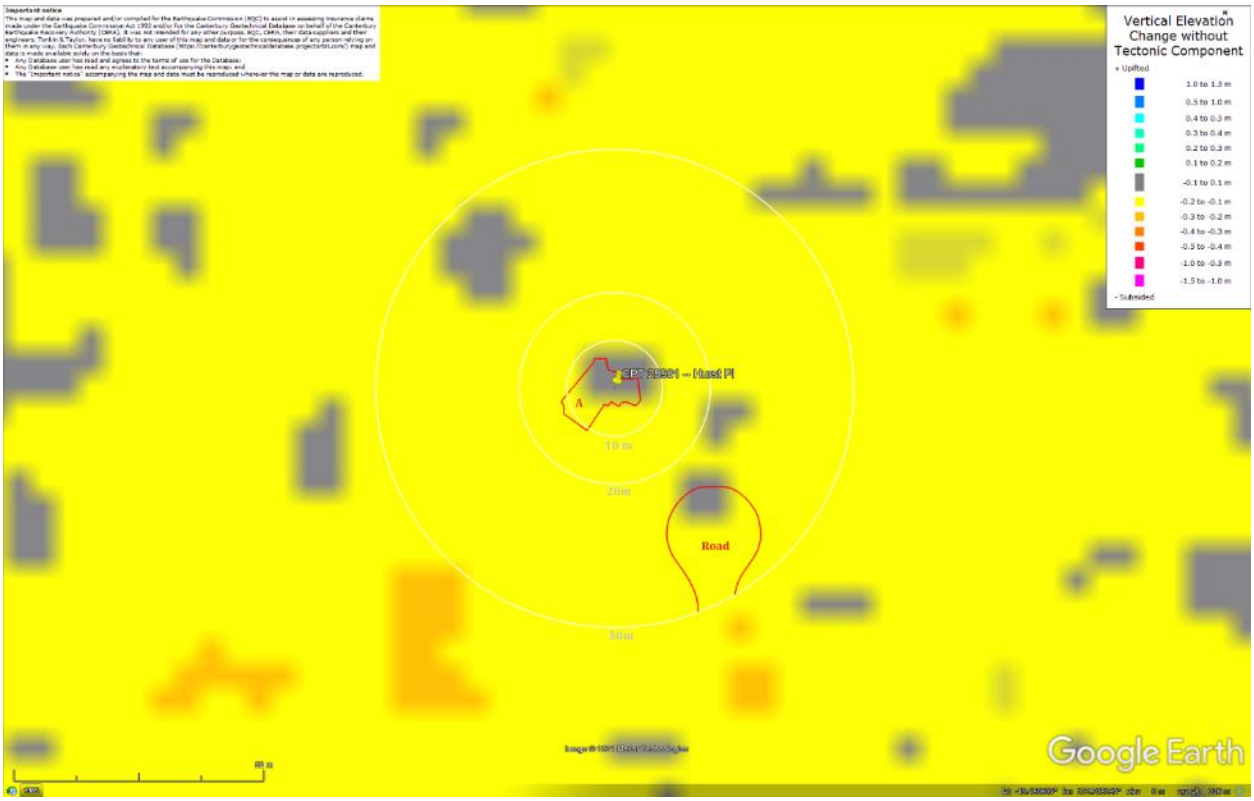

Figure 30: Ground surface subsidence without tectonic component for June 2011 Earthquake according to the LiDAR DEM.

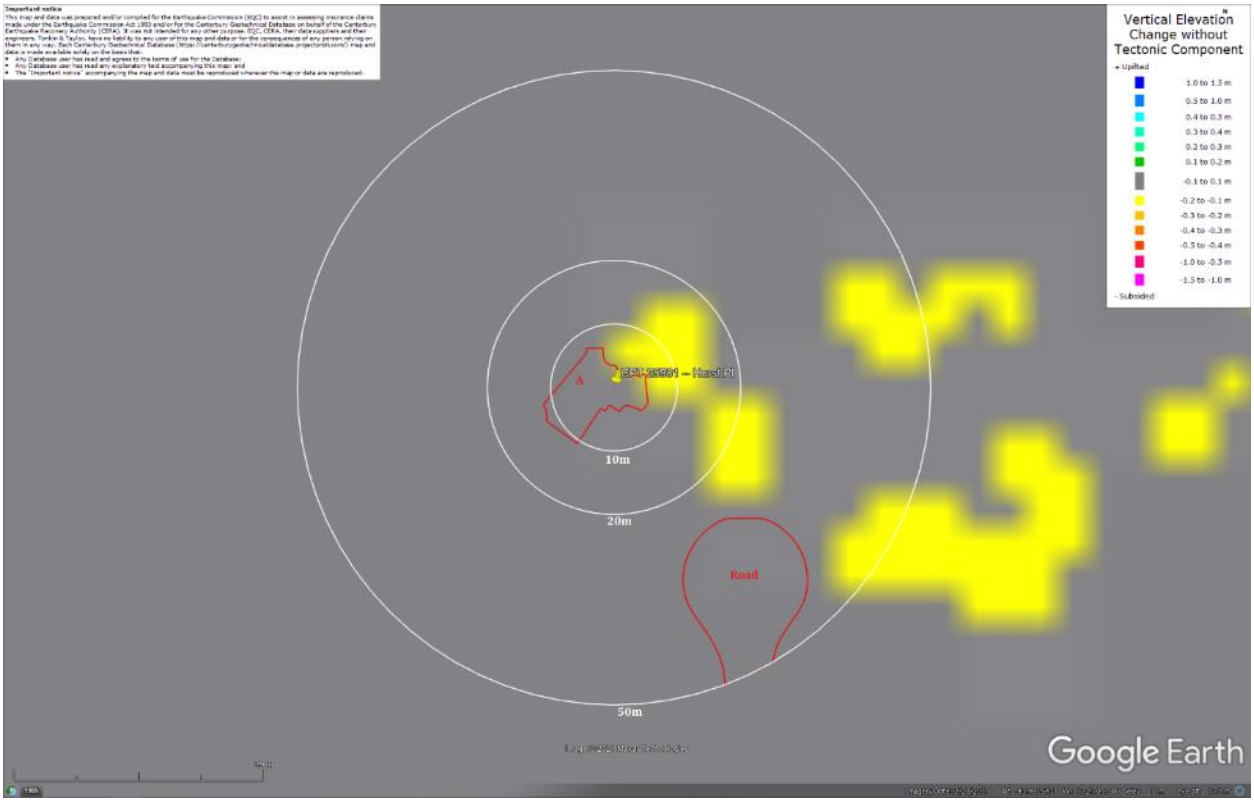

Figure 31: Ground surface subsidence without tectonic component for Dec 2011 Earthquake according to the LiDAR DEM.

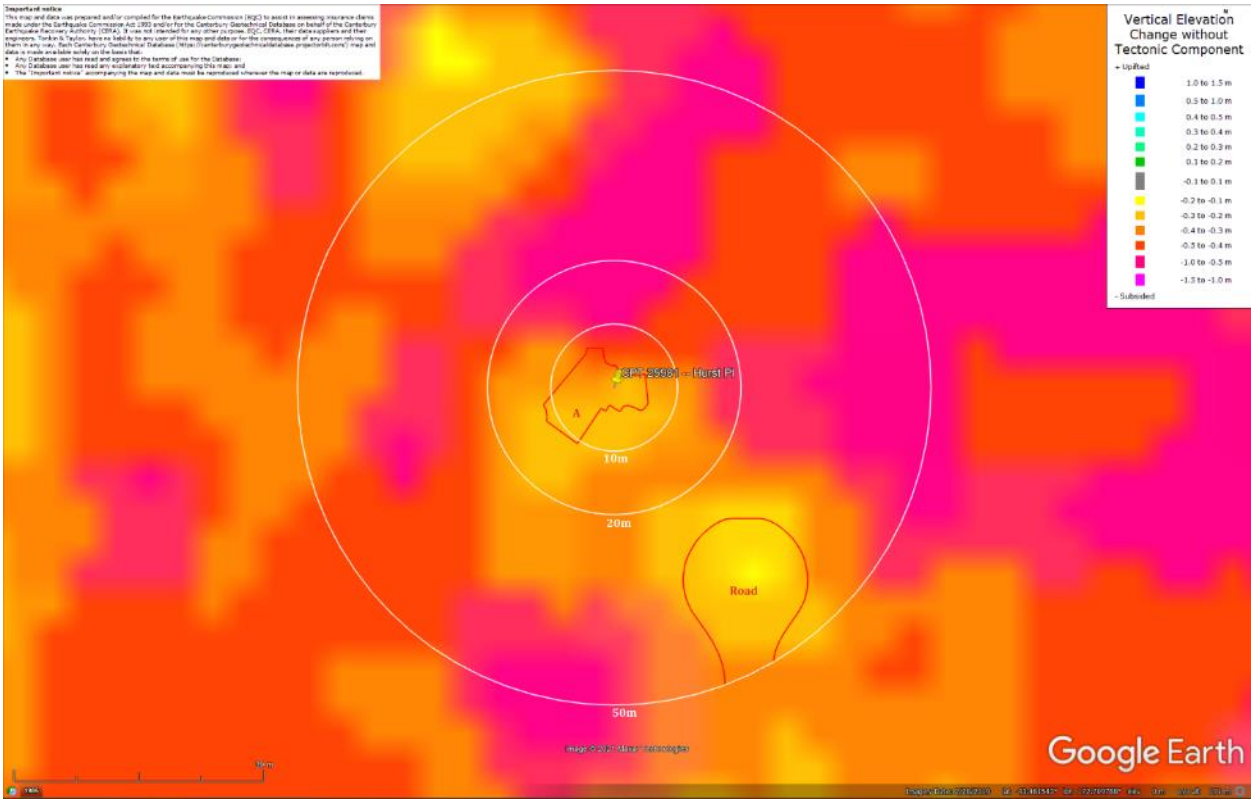

Figure 32: Ground surface subsidence without tectonic component for Canterbury Earthquake Sequence according to the LiDAR DEM.

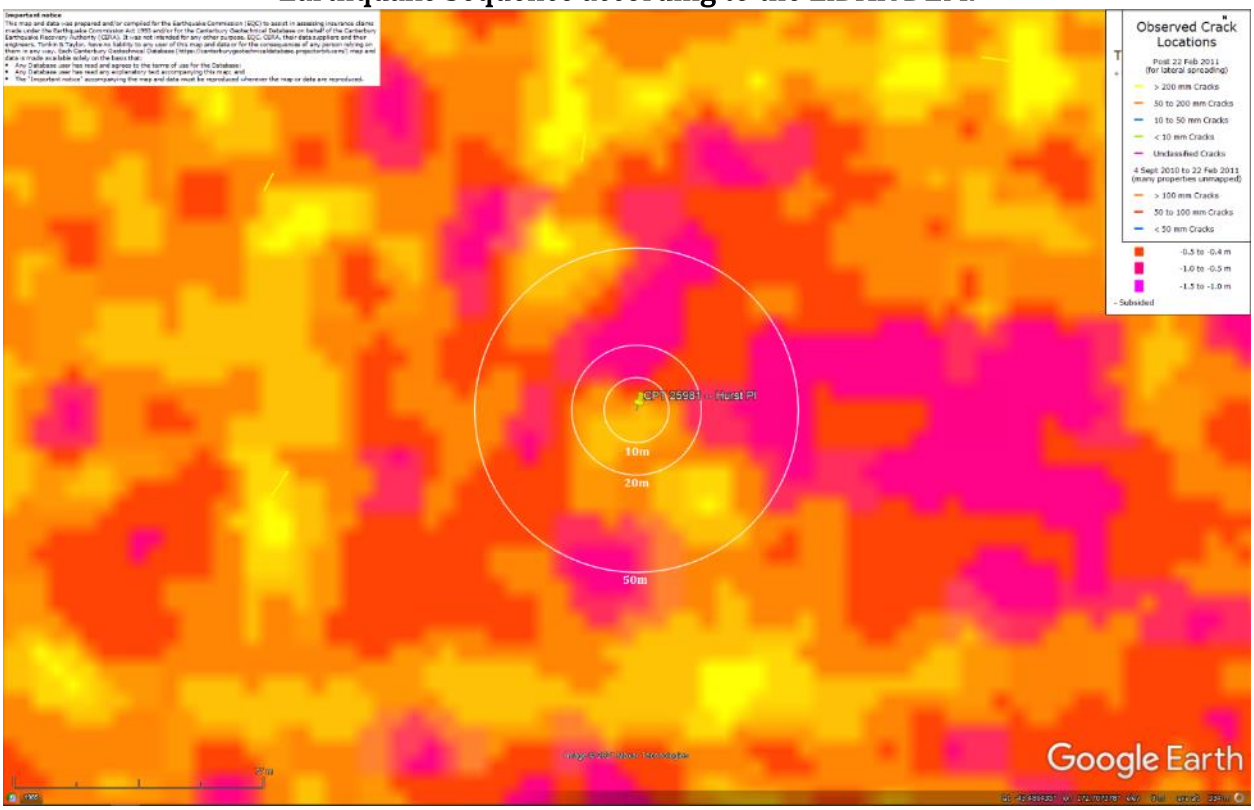

Figure 33: No lateral spreading for Canterbury Earthquake Sequence.

Figure 34: Vertical tectonic movements for Sep 2010 Earthquake.

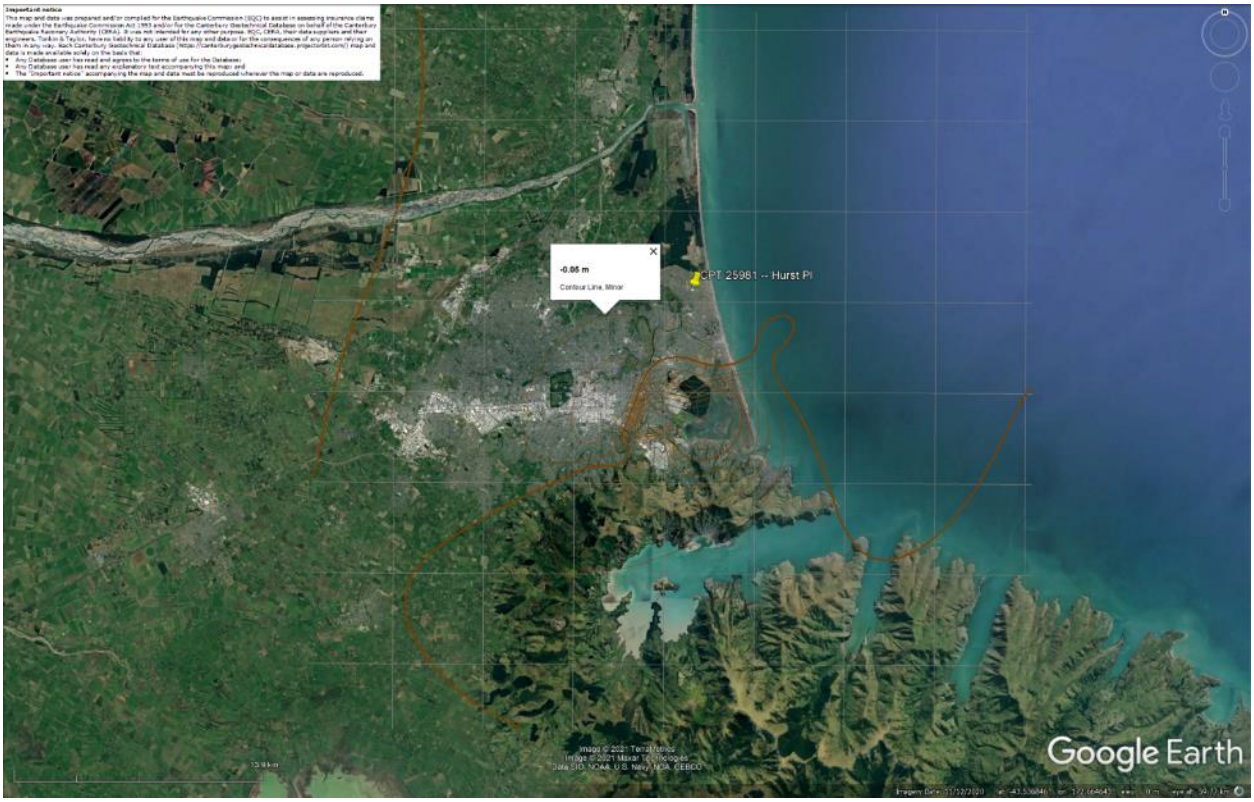

Figure 35: Vertical tectonic movements for Feb 2011 Earthquake.

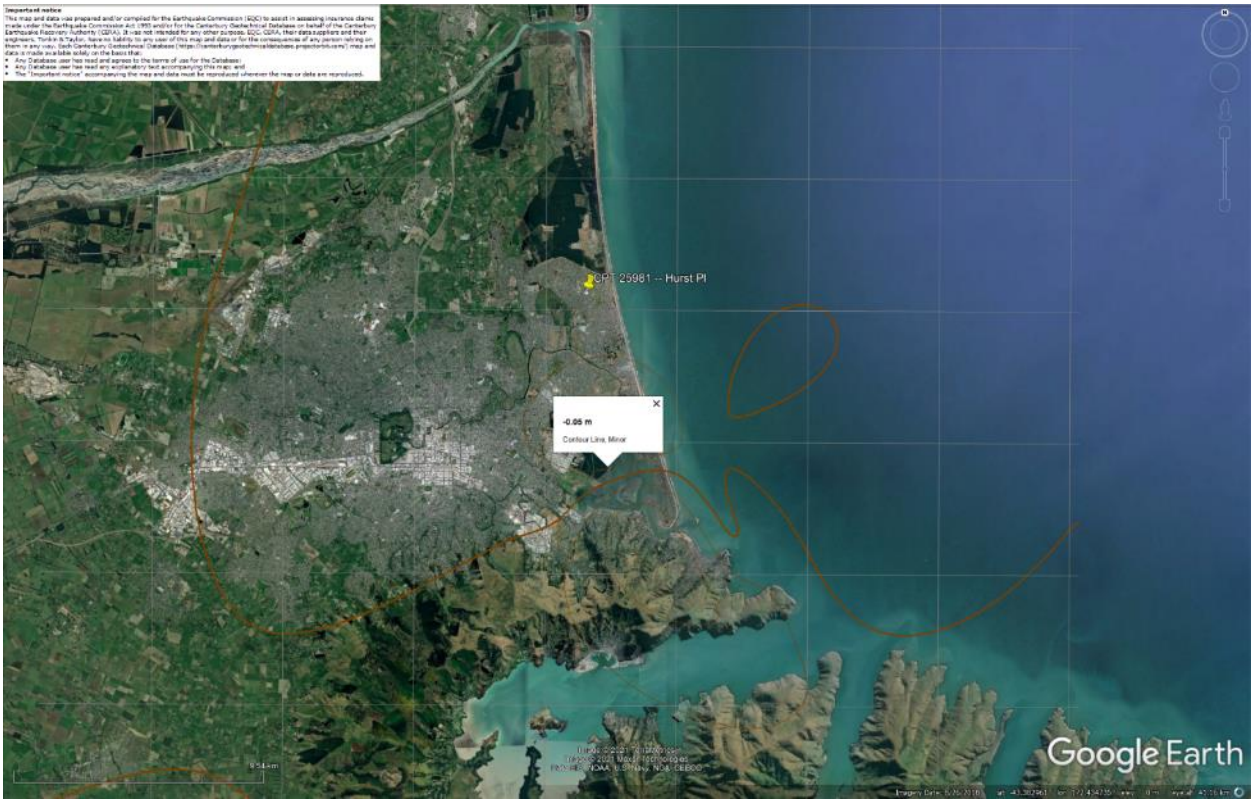

Figure 36: Vertical tectonic movements for June 2011 Earthquake.

Figure 37: Vertical tectonic movements for Dec 2011 Earthquake.

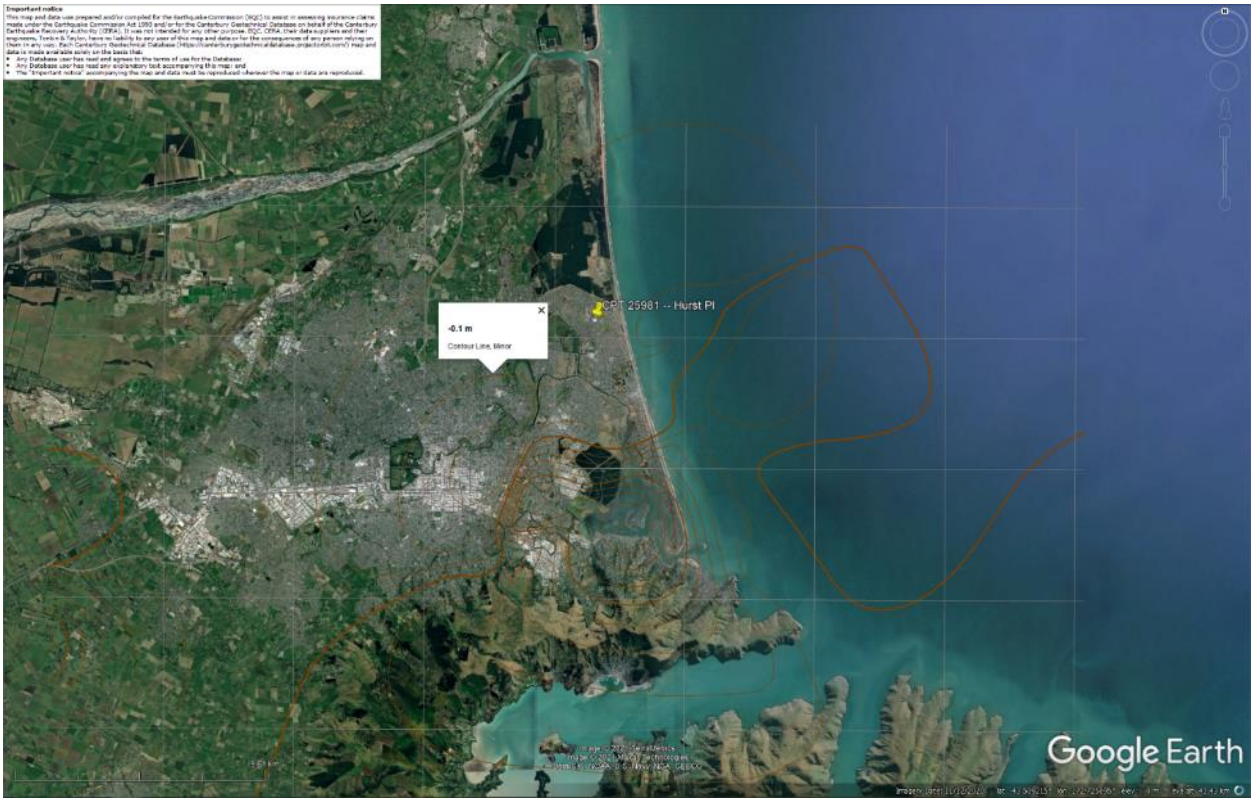

Figure 38: Vertical tectonic movements for Canterbury Earthquake Sequence.

Figure 39: Aerial photograph showing the ejecta outline at the site for Feb-11 EQ.

Figure 40: Aerial photograph acquired on 16 Jun 2011 showing the ejecta outline at the site for Jun-11 EQ.

Figure 41: Aerial photograph showing the ejecta outline at the site for Dec-11 EQ.

Contents of this figure cannot be shared as doing so is restricted by a Non-Disclosure Agreement.

Figure 42: LDAT inspection notes for the property with Patch A (inspection date: July 2011).

Figure 43: Ground photographs showing ejecta remnants at the property with Patch A (photograph date: July 2011).

Figure 44: Ground photographs showing ejecta remnants at the properties within the 50-m buffer (photograph date: July 2011).

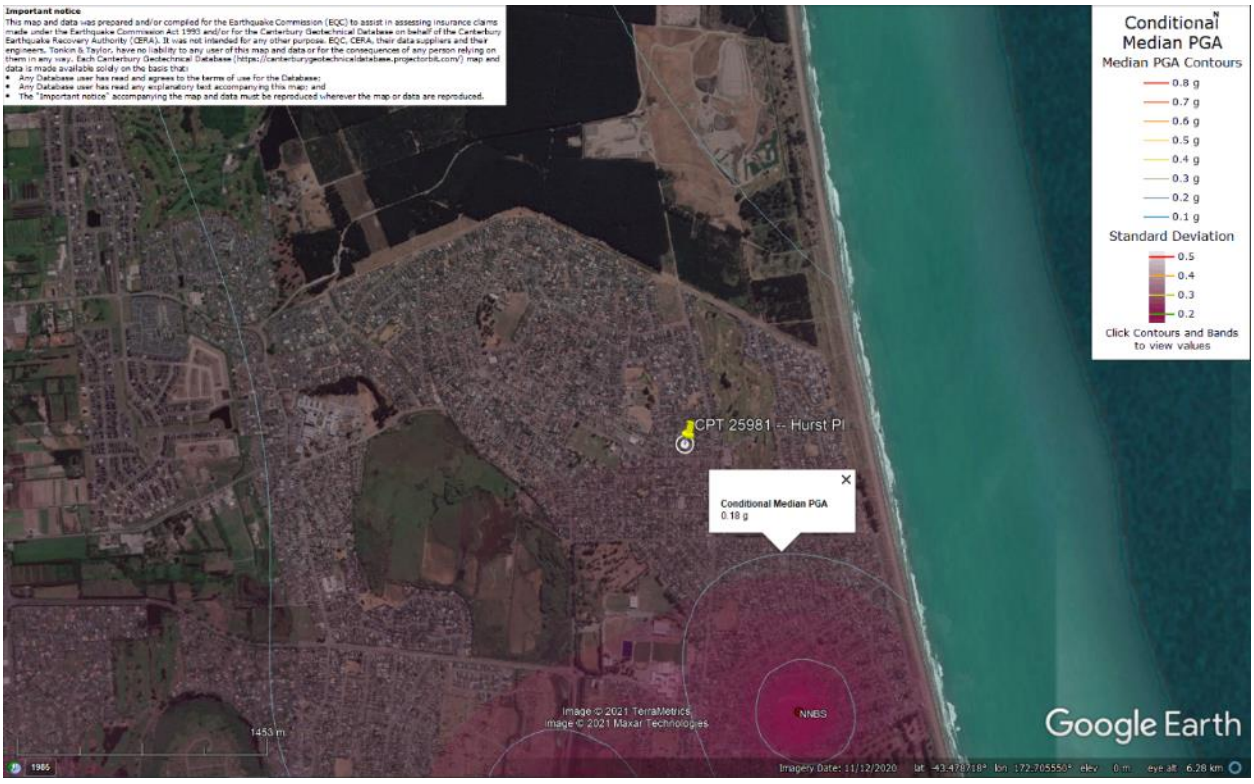

Figure 45: PGA for Sep-10 EQ (st. dev. = 0.325-0.375 ln units).

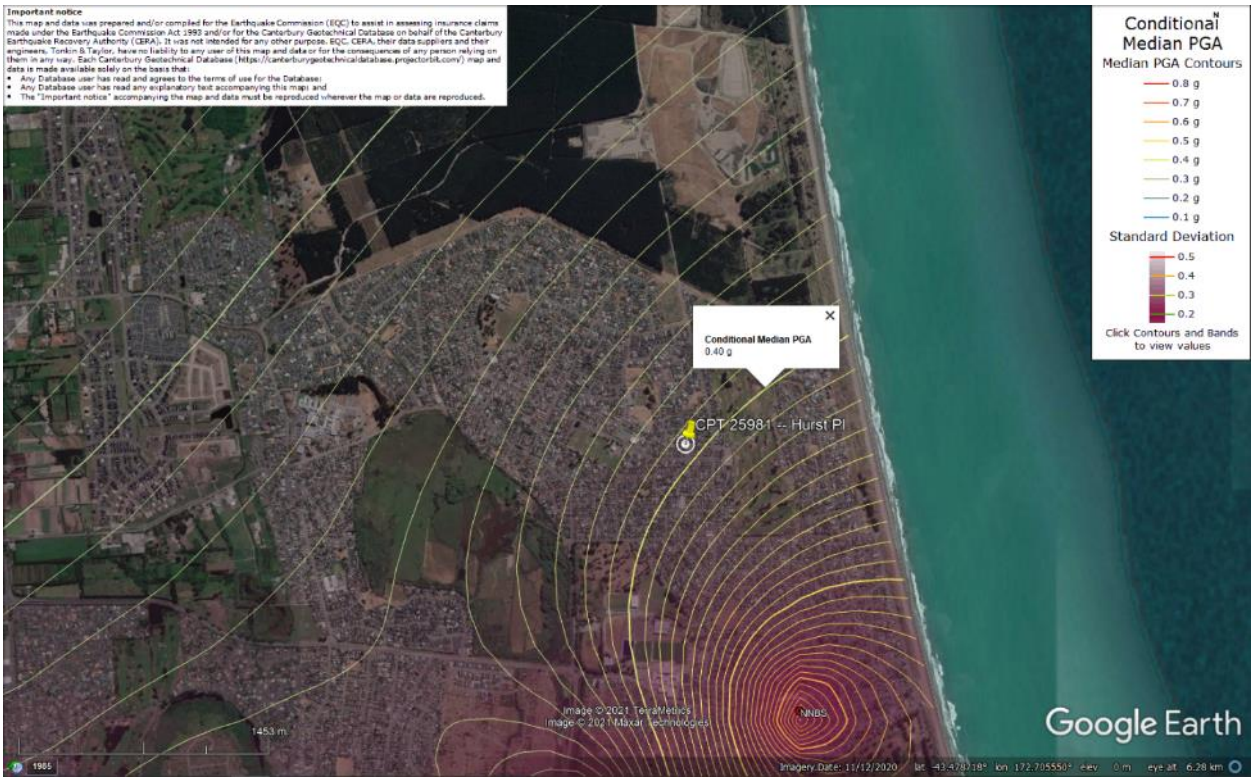

Figure 46: PGA for Feb-11 EQ (st. dev. = 0.350-0.400 ln units).

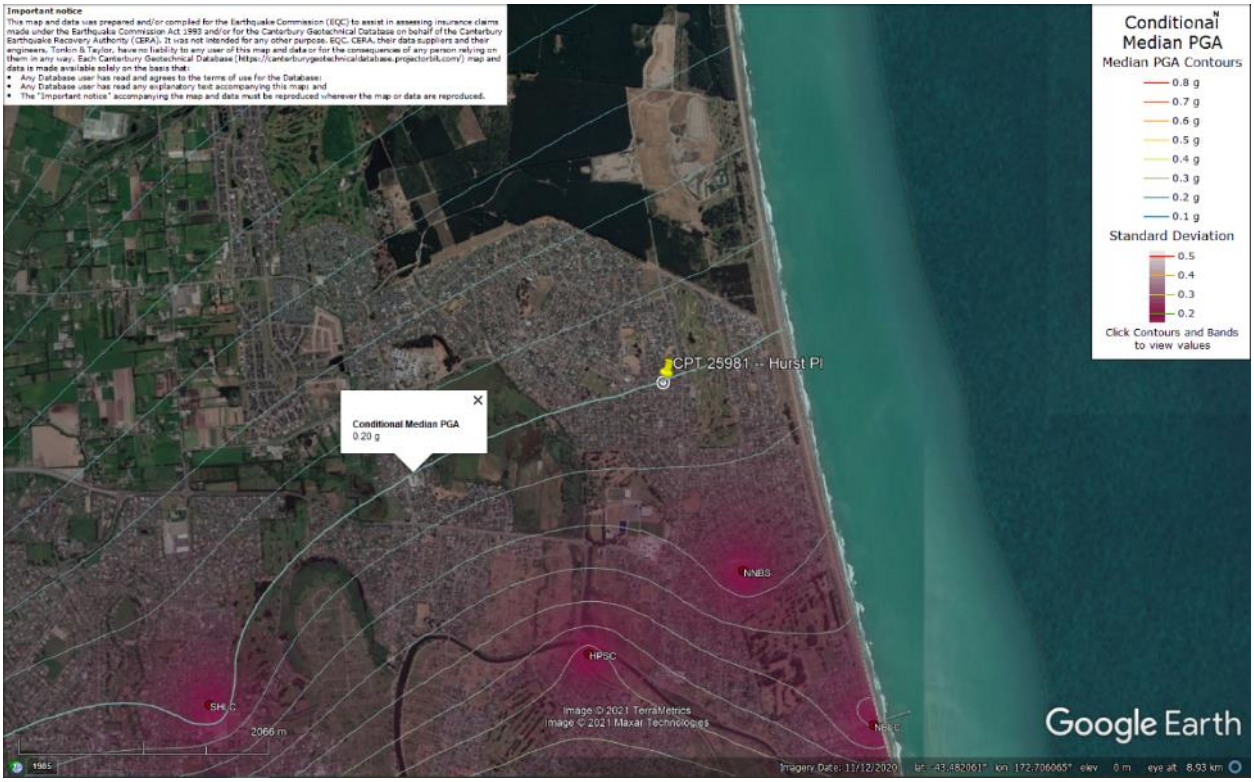

Figure 47: PGA for Jun-11 EQ (st. dev. = 0.375-0.400 ln units).

Figure 48: PGA for Dec-11 EQ (st. dev. = 0.400-0.425 ln units).

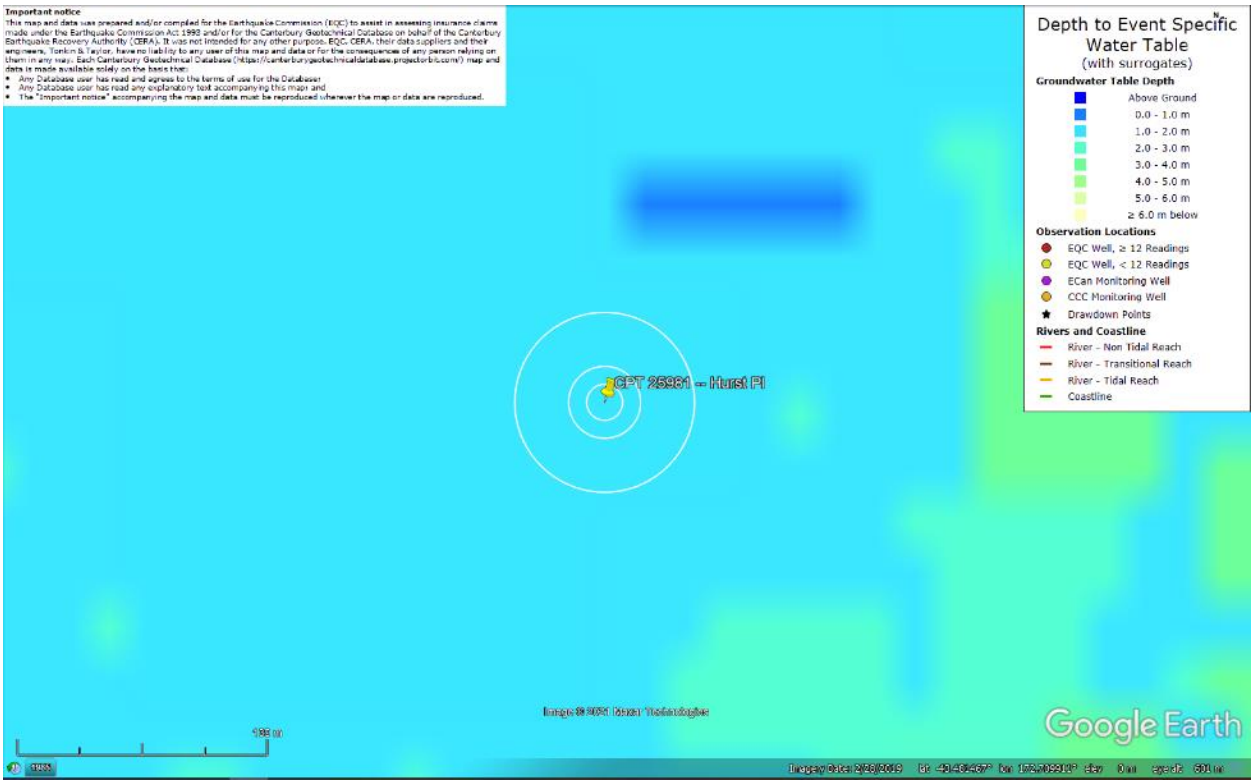

Figure 49: Depth to groundwater table for Sep-10 EQ.

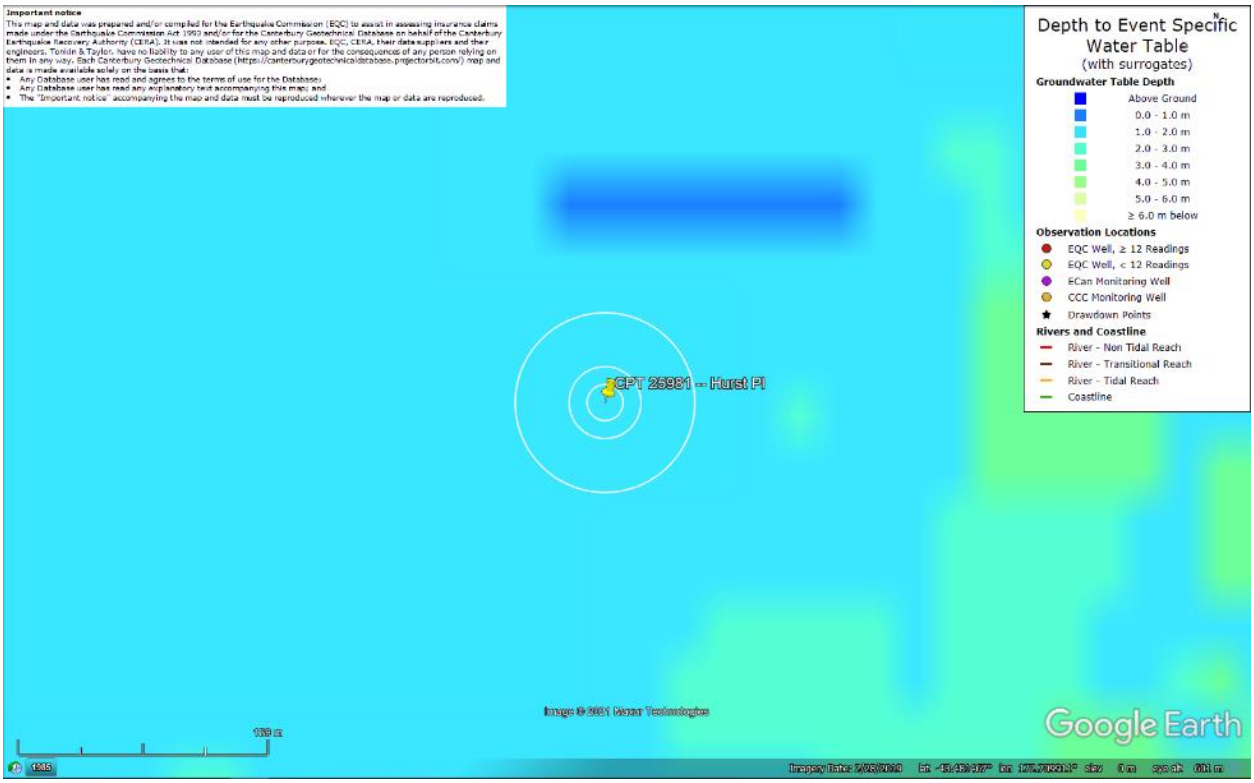

Figure 50: Depth to groundwater table for Feb-11 EQ.

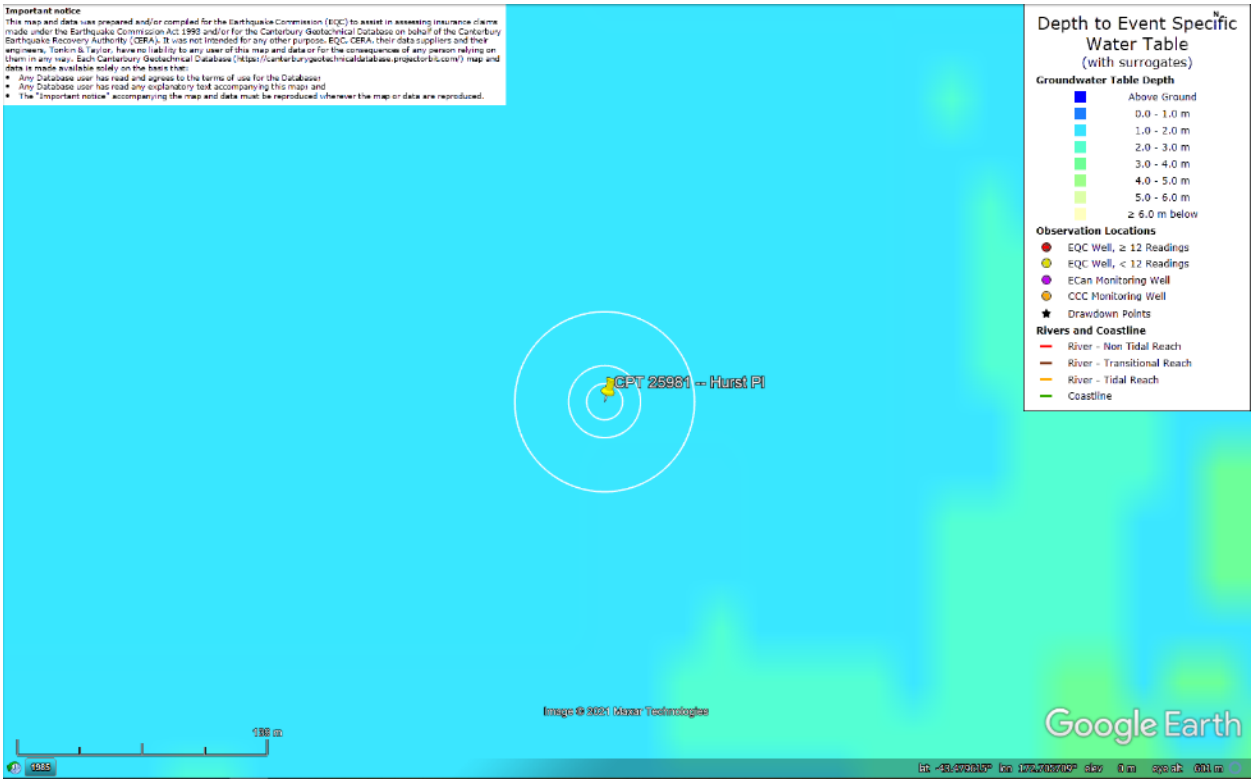

Figure 51: Depth to groundwater table for Jun-11 EQ.

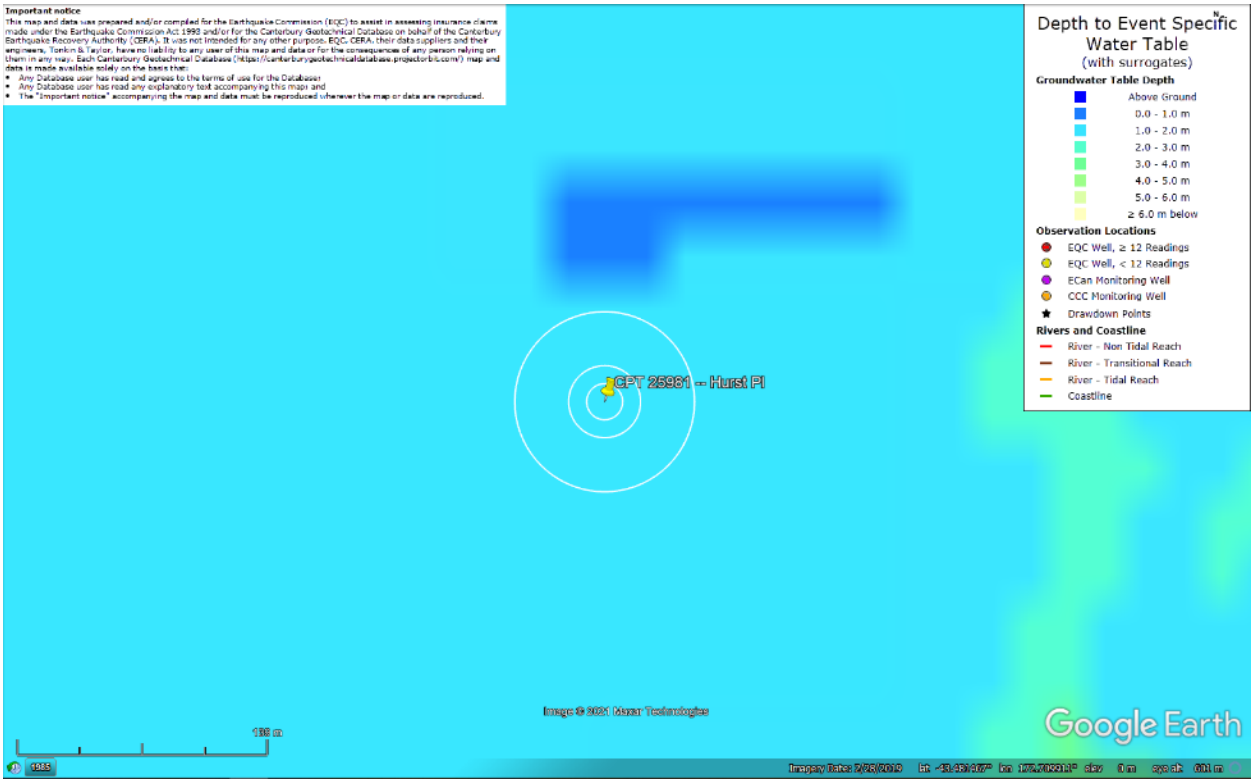

Figure 52: Depth to groundwater table for Dec-11 EQ.

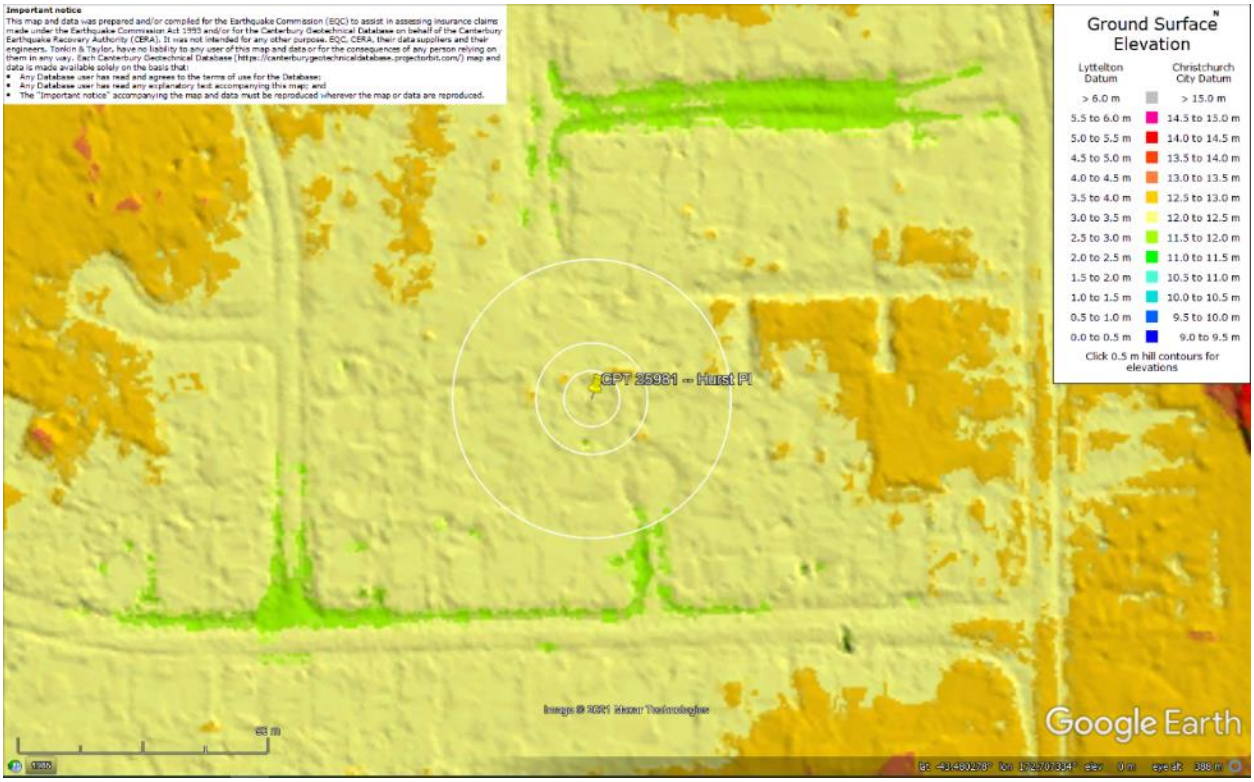

Figure 53: Ground surface elevation according to the Sep-11 LiDAR survey.

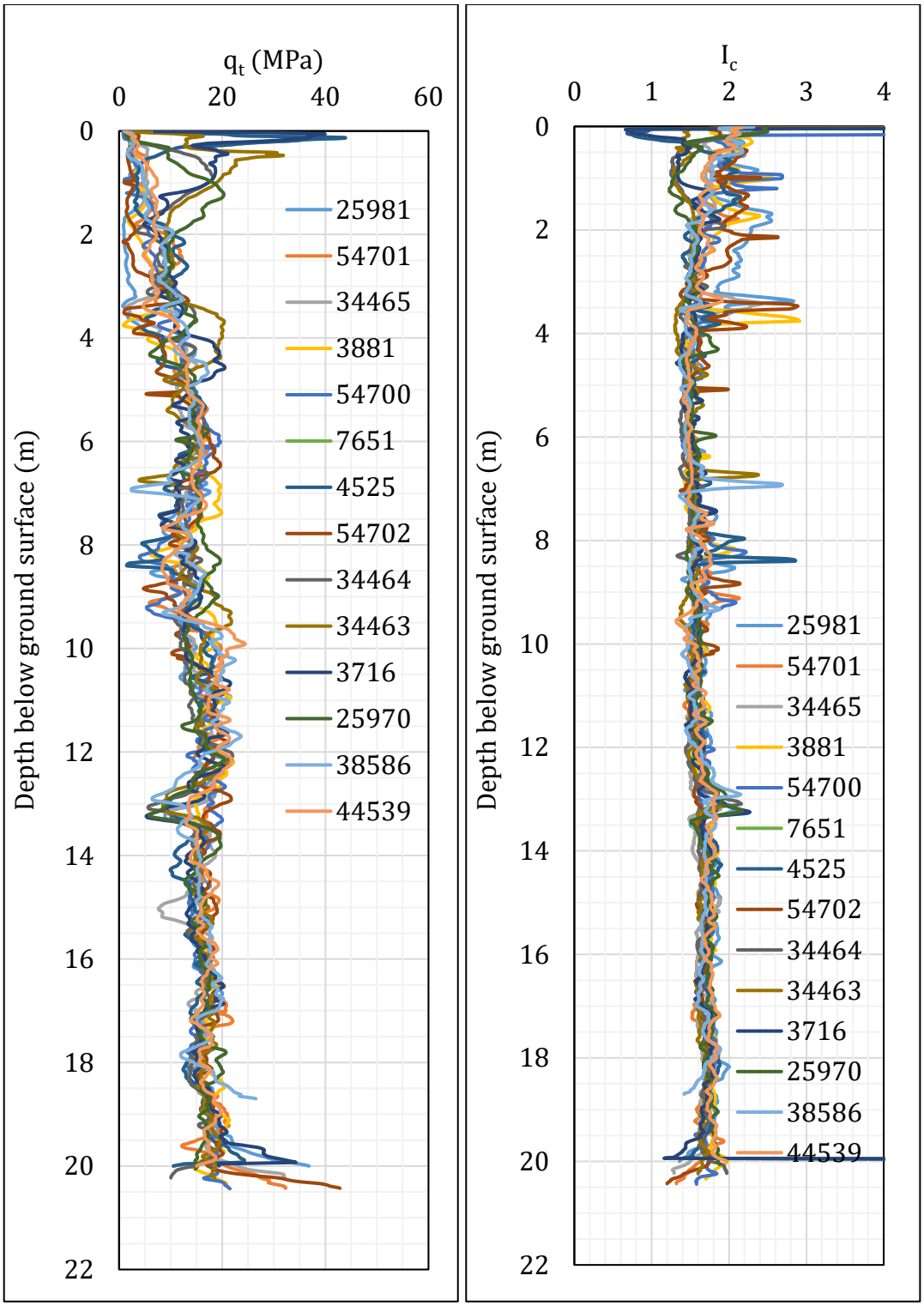

Figure 54: q_t and I_c profiles.

Note 5: The selection of CPTs for the area considered for settlement assessment (Figure 1) is based on the proximity of the CPTs to the considered areas. In accordance with that, the following table shows CPTs that were used for the volumetric settlement analysis in *Cliq v.3.0.3.2*, a CPT soil liquefaction software developed by GeoLogismiki. (The average volumetric settlements were reported in Table 8.)

Table 12: CPT profiles used in volumetric settlement analysis for areas selected for settlement assessment.

CPT ID No.	Patch A	Road
25981	✓	
54701		
34465		
3881		✓
54700		
7651		✓
4525		
54702		
34464		
34463		
3716		
25970		
38586		
44539		✓

Table 13a: CPT-based results.

EQ Event	Parameter	CPT ID 25981	54701	34465	3881	54700	7651	4525	54702
Sep-10	S_{V1D} (mm)	32	3	16	5	9	11	9	12
	LSN	11	0	3	1	1	2	3	4
	LPI	1	0	0	0	0	0	0	0
	LPI_{ish}	0	0	0	0	0	0	0	0
	$D_{FS<1}$ (m)	2.48	undet.	undet.	undet.	undet.	undet.	undet.	undet.
Feb-11	S_{V1D} (mm)	92	60	134	47	75	114	89	99
	LSN	30	9	21	17	14	17	24	27
	LPI	12	3	9	5	6	8	9	10
	LPI_{ish}	12	1	5	6	3	3	8	10
	$D_{FS<1}$ (m)	1.52	2.85	1.51	1.56	1.81	1.51	1.51	1.51
Jun-11	S_{V1D} (mm)	38	2	11	5	7	8	9	10
	LSN	13	0	2	1	1	1	3	4
	LPI	1	0	0	0	0	0	0	0
	LPI_{ish}	0	0	0	0	0	0	0	0
	$D_{FS<1}$ (m)	2.08	undet.	undet.	undet.	undet.	undet.	3.53	undet.
Dec-11	S_{V1D} (mm)	83	34	94	39	51	77	65	77
	LSN	29	5	16	14	10	12	20	24
	LPI	9	2	5	4	3	5	5	7
	LPI_{ish}	8	1	4	4	2	3	5	7
	$D_{FS<1}$ (m)	1.54	8.34	1.51	1.64	2.22	3.46	1.53	1.51

Notes: $D_{FS<1}$ = Depth to the first liquefiable layer ($FS_L<1$) that is at least 200-mm thick, as determined by the Boulanger and Idriss (2016) liquefaction-triggering procedure (P_L=50%, C_{FC}=0.13, and $I_{c,cutoff}$ =2.6), and exported from *Cliq v.3.0.3.2*; undet. = the specified soil layer was not detected.

Table 13b: CPT-based results (continued).

EQ Event	Parameter	CPT ID 34464	34463	3716	25970	38586	44539
Sep-10	S_{V1D} (mm)	12	3	5	2	4	8
	LSN	1	0	1	0	0	1
	LPI	0	0	0	0	0	0
	LPI_{ish}	0	0	0	0	0	0
	$D_{FS<1}$ (m)	13.17	undet.	undet.	undet.	undet.	8.52
Feb-11	S_{V1D} (mm)	148	96	96	42	66	67
	LSN	19	10	12	5	10	18
	LPI	7	5	5	2	3	7
	LPI_{ish}	4	0	0	0	2	5
	$D_{FS<1}$ (m)	1.66	5.10	6.55	4.12	1.51	1.70
Jun-11	S_{V1D} (mm)	5	1	3	1	2	5
	LSN	1	0	0	0	0	1
	LPI	0	0	0	0	0	0
	LPI_{ish}	0	0	0	0	0	0
	$D_{FS<1}$ (m)	undet.	undet.	undet.	undet.	undet.	undet.
Dec-11	S_{V1D} (mm)	98	56	59	26	39	52
	LSN	13	6	7	3	6	13
	LPI	3	2	2	1	2	4
	LPI_{ish}	2	1	1	0	1	2
	$D_{FS<1}$ (m)	1.69	6.44	7.12	4.18	1.58	2.10

Notes: $D_{FS<1}$ = Depth to the first liquefiable layer ($FS_L<1$) that is at least 200-mm thick, as determined by the Boulanger and Idriss (2016) liquefaction-triggering procedure (P_L=50%, C_{FC}=0.13, and $I_{c,cutoff}$ =2.6), and exported from *Cliq v.3.0.3.2*; undet. = the specified soil layer was not detected.

Note 6: Based on the borehole log (BH 4950, Figure 1), the groundwater table is at a depth of 1.95 m below the ground surface. The soil profile consists of (1) gravelly fine to medium sand, SW, as fill underlying asphalt to a depth of 0.25 m and (2) and fine to medium sand, SP, of the Christchurch formation, to a depth of 20 m.

Note 7: The ejecta-induced free-field settlement provided in Table 11 is an areal average settlement due to ejecta, which is based on the total settlement assessment area, A_T (provided in Table 9 and repeated in Table 14). However, the considered area was not always covered completely with ejecta; thus, it is important to provide the localized ejecta-induced settlement, too. The localized settlement due to ejecta is estimated using photographic evidence only as

$$S_{E,P\_localized} = \frac{V_E}{A_E}$$

where V_E is the total volume of ejecta within A_T and A_E is the total coverage area of ejecta within A_T. Please note that the areal ejecta-induced settlement provided in Table 14 as S_{E,P_areal} is the same as $S_{E,P}$ in Table 11, which was estimated as

$$S_{E,P\_areal} = S_{E,P} = \frac{V_E}{A_T}$$

where V_E is the total volume of ejecta within A_T and A_T is the total settlement assessment area.

Table 14a: Areal and localized ejecta-induced settlement estimates for Patch A based on photographic evidence.

Earthquake Event	A_T (m^2)	A_E (m^2)	V_E (m^3)	S_{E,P_areal} (mm)	$S_{E,P\_localized}$ (mm)
Sep-10	125	0	0	0	0
Feb-11	125	115	6.0-9.3	60±15	65±15
Jun-11	108	64.7	1.9-3.9	*25±10	*45±15
Dec-11	122	77.9	2.8-4.4	30±5	45±10

Notes: S_{E,P_areal} = $S_{E,P}$ reported in Table 11 = areal ejecta-induced settlement; $S_{E,P\_localized}$ = localized ejecta-induced settlement; A_T = total settlement assessment area; V_E = total volume of ejecta within A_T; A_E = total area of ejecta within A_T; The estimates of both areal and localized ejecta-induced settlement are rounded to the nearest 5; Final plus/minus values are also rounded to the nearest 5; * indicates uncertainty due to the presence of shadows.

Table 14b: Areal and localized ejecta-induced settlement estimates for Road based on photographic evidence.

Earthquake Event	A_T (m^2)	A_E (m^2)	V_E (m^3)	S_{E,P_areal} (mm)	$S_{E,P\_localized}$ (mm)
Sep-10	357	0	0	0	0
Feb-11	357	357	18.7-21.3	55±5	55±5
Jun-11	357	357	9.0-18.0	40±10	40±10
Dec-11	357	ND	ND	ND	ND

Notes: S_{E,P_areal} = $S_{E,P}$ reported in Table 11 = areal ejecta-induced settlement; $S_{E,P\_localized}$ = localized ejecta-induced settlement; A_T = total settlement assessment area; V_E = total volume of ejecta within A_T; A_E = total area of ejecta within A_T; The estimates of both areal and localized ejecta-induced settlement are rounded to the nearest 5; Final plus/minus values are also rounded to the nearest 5; ND = Not determined.

Summary 2:

- **The best estimate of the localized ejecta-induced free-field ground settlement at the Hurst Pl site for the SEP 2010, FEB 2011, JUN 2011, and DEC 2011 earthquake is 0 mm, 65±15 mm, 45±15 mm, and 45±10 mm, respectively.**
- **The best estimate of the localized ejecta-induced free-field settlement of the road at the Hurst Pl site for the SEP 2010, FEB 2011, and JUN 2011 earthquake is 0 mm, 55±5 mm, and 40±10 mm, respectively. The localized ejecta-induced settlement of the road for the DEC 2011 earthquake could not be estimated with confidence.**